Inorganic Chemistry

Article

pubs.acs.org/IC

Gold(I) and Related Heterometallic Derivatives of Dimolybdenum Complexes with Asymmetric Phosphinidene Bridges

Belén Alvarez, M. Angeles Alvarez, Inmaculada Amor, M. Esther García,* Miguel A. Ruiz,* and Jaime Suárez

Departamento de Química Orgánica e Inorgánica/IUQOEM, Universidad de Oviedo, E-33071 Oviedo, Spain

Supporting Information

ABSTRACT: The phosphinidene-bridged complexes $[Mo_2Cp_2(\mu\text{-}\kappa^1{:}\kappa^1,\eta^6\text{-PR*})(CO)_2]$ (**1**), $[Mo_2Cp_2(\mu\text{-}\kappa^1{:}\kappa^1,\eta^4\text{-PR*})(CO)_3]$ (**2**), $[Mo_2Cp(\mu\text{-}\kappa^1{:}\kappa^1,\eta^5\text{-}PC_5H_4)(\eta^6\text{-HR*})(CO)_2]$ (**3**), and $[Mo_2Cp_2(\mu\text{-}\kappa^1{:}\kappa^1\text{-PH})(\eta^6\text{-HR*})(CO)_2]$ (**4**) were examined as precursors of heterometallic gold(I) and related derivatives (Cp = η^5-C_5H_5, R* = 2,4,6-$C_6H_2{}^tBu_3$). These complexes reacted with [AuCl(THT)] to give the corresponding derivatives $[AuMo_2ClCp_2(\mu\text{-}\kappa^1{:}\kappa^1{:}\kappa^1,\eta^6\text{-PR*})(CO)_2]$, $[AuMo_2ClCp_2(\mu\text{-}\kappa^1{:}\kappa^1{:}\kappa^1,\eta^4\text{-PR*})(CO)_3]$ (Au−Mo = 2.8493(6) Å), $[AuMo_2ClCp(\mu\text{-}\kappa^1{:}\kappa^1{:}\kappa^1,\eta^5\text{-}PC_5H_4)(CO)_2(\eta^6\text{-HR*})]$, and $[AuMo_2ClCp_2(\mu_3\text{-PH})(CO)_2(\eta^6\text{-HR*})]$ formally resulting from the addition of an acceptor AuCl moiety to the short Mo−P bond of the parent substrates almost perpendicular to the corresponding Mo_2P plane. The chloride ligand was easily displaced upon reaction of the PC_5H_4-bridged gold complex with $K[MoCp(CO)_3]$ to give the tetranuclear derivative $[AuMo_3Cp_2(\mu\text{-}\kappa^1{:}\kappa^1{:}\kappa^1,\eta^5\text{-}PC_5H_4)(CO)_5(\eta^6\text{-HR*})]$ (Au−Mo = 2.711(2) and 2.807(2) Å). Compound **1** also reacted with HgI_2 to give a hexanuclear complex $[HgMo_2Cp_2(\mu\text{-I})I(\mu\text{-}\kappa^1{:}\kappa^1,\eta^6\text{-PR*})(CO)_2]_2$ containing dative Mo→Hg bonds (2.820(1) and 2.827(1) Å), whereas complex **3** gave the μ_3-PR bridged complex $[HgMo_2CpI_2(\mu\text{-}\kappa^1{:}\kappa^1{:}\kappa^1,\eta^5\text{-}PC_5H_4)(CO)_2(\eta^6\text{-HR*})]$. Complexes **1** to **4** also reacted easily with $[AuL(THT)]PF_6$ (L = THT, P(*p*-tol)$_3$, PMe_3, P^iPr_3) to give the corresponding cationic trinuclear derivatives $[AuMo_2Cp_2(\mu\text{-}\kappa^1{:}\kappa^1{:}\kappa^1,\eta^6\text{-PR*})(CO)_2L](PF_6)$ (Au−Mo = 2.8080(3) Å for L = P(*p*-tol)$_3$), $[AuMo_2Cp_2(\mu\text{-}\kappa^1{:}\kappa^1{:}\kappa^1,\eta^4\text{-PR*})(CO)_3L](PF_6)$, and $[AuMo_2Cp(\mu\text{-}\kappa^1{:}\kappa^1{:}\kappa^1,\eta^5\text{-}PC_5H_4)(CO)_2(\eta^6\text{-HR*})\{P(p\text{-tol})_3\}](PF_6)$. The blue, analogous PH-bridged complexes were more conveniently isolated as tetraarylborate salts $[AuMo_2Cp_2(\mu_3\text{-PH})(CO)_2(\eta^6\text{-HR*})L](BAr'_4)$ (Au−Mo = 2.8038(6) Å for L = P^iPr_3; Ar′= 3,5-$C_6H_3(CF_3)_2$]. Compounds **1**, **3**, and **4** reacted readily with the cation $[Au(THT)_2]^+$ (as PF_6^- or $BAr'_4{}^-$ salts) in a 2:1 ratio to give respectively the corresponding pentanuclear derivatives $[Au\{Mo_2Cp_2(\mu\text{-}\kappa^1{:}\kappa^1{:}\kappa^1,\eta^6\text{-PR*})(CO)_2\}_2](PF_6)$, $[Au\{Mo_2Cp(\mu\text{-}\kappa^1{:}\kappa^1{:}\kappa^1,\eta^5\text{-}PC_5H_4)(CO)_2(\eta^6\text{-HR*})\}_2](PF_6)$ (Au−Mo = 2.7975(7) and 2.8006(7) Å), and $[Au\{Mo_2Cp_2(\mu_3\text{-PH})(CO)_2(\eta^6\text{-HR*})\}_2](BAr'_4)$ (Au−Mo = 2.8233(8) and 2.8691(7) Å). Related silver complexes were obtained from the reaction of **3** and **4** with $[AgCl(PPh_3)]_4$ after spontaneous symmetrization, while reaction of **1** with $[Cu(NCMe)_4]PF_6$ in a 2:1 ratio yielded the analogous copper complex $[Cu\{Mo_2Cp_2(\mu\text{-}\kappa^1{:}\kappa^1{:}\kappa^1,\eta^6\text{-PR*})(CO)_2\}_2](PF_6)$. All the above cationic gold complexes having $(\mu\text{-}\kappa^1{:}\kappa^1{:}\kappa^1,\eta^6\text{-PR*})$ ligands (but not the copper complex) rearranged into $[Au\{Mo_2Cp(\mu\text{-}\kappa^1{:}\kappa^1{:}\kappa^1,\eta^5\text{-}PC_5H_4)(CO)_2(\eta^6\text{-HR*})\}_2](PF_6)$ in refluxing 1,2-dichloroethane solution.

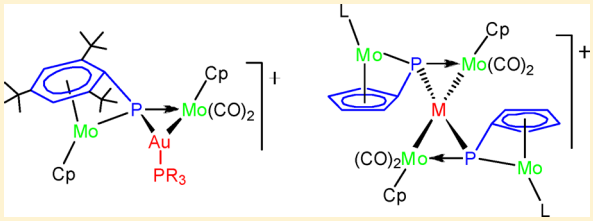

INTRODUCTION

The chemistry of gold complexes and clusters is a matter of current interest not only because of particular aspects of the structure and bonding in these species, including aurophilic interactions,[1] but also because of their photophysical and photochemical properties[2] and their remarkable catalytic activity in many organic reactions.[3] Extensive work has been carried out also on the synthesis and properties of mixed transition metal−gold compounds,[4] although several types of complexes remain relatively unexplored to date, these including heterometallic gold compounds stabilized by phosphinidene (PR) bridging ligands. Although the latter ligands have long been known as good supporting ligands for transition-metal clusters because of their ability to bind up to four metal atoms simultaneously,[5] their use in stepwise and rational synthesis of heterometallic clusters has been limited so far to a few binuclear species.

When bridging two metal atoms, the phosphinidene ligand may display three different coordination modes, depending on the electronic demands of the metal fragments involved (Chart 1). Complexes of type **C** are obvious potential donors to unsaturated or labile metal complexes (hence useful precursors for heterometallic derivatives) due to the presence of a lone

Chart 1

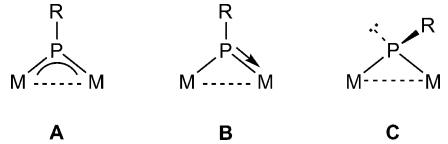

Received: June 11, 2014
Published: September 5, 2014

dx.doi.org/10.1021/ic501376v | *Inorg. Chem.* 2014, 53, 10325−10339

pair at the pyramidal phosphorus atom of the PR ligand. Indeed, some transient anionic complexes of type **C**,[6−8] as well as the isolable neutral complexes $[Fe_2Cp_2(\mu\text{-PR})(\mu\text{-CO})(CO)_2]$,[9] have been used to build up different heterometallic gold complexes bridged by phosphinidene ligands. Complexes of types **A** and **B** also are potential donors to unsaturated metal centers via their π(Mo−P) bonding electron pair. Out of these, type **A** complexes are expected to be less efficient donors, because of the full delocalization of this bonding pair along the M−P−M chain. Indeed, their reactions with different transition metal complexes are often complex and far from simple addition of an unsaturated fragment to the dimetal substrate.[10] Moreover, no reactions with gold complexes appear to have been studied so far for these substrates. In contrast, type **B** complexes display π electron density more concentrated at the short Mo−P bond and are thus expected to be more efficient donors toward unsaturated metal centers. We have previously reported and studied some chemistry of four dimolybdenum complexes of type **B**, these having either bifunctional arylphosphinidene ($[Mo_2Cp_2(\mu\text{-}\kappa^1{:}\kappa^1,\eta^6\text{-PR*})(CO)_2]$ (**1**), $[Mo_2Cp_2(\mu\text{-}\kappa^1{:}\kappa^1,\eta^4\text{-PR*})(CO)_3]$ (**2**)),[11] cyclopentadienylidene-phosphinidene ($[Mo_2Cp(\mu\text{-}\kappa^1{:}\kappa^1,\eta^5\text{-}PC_5H_4)(\eta^6\text{-HR*})(CO)_2]$ (**3**)),[11] or bare phosphinidene ligands ($[Mo_2Cp_2(\mu\text{-}\kappa^1{:}\kappa^1\text{-PH})(\eta^6\text{-HR*})(CO)_2]$ (**4**)),[12] respectively (Chart 2; Cp = η^5-C_5H_5, R* = 2,4,6-$C_6H_2{}^tBu_3$). According to DFT calculations, the Mo−P π interaction is strictly localized on the short Mo−P bond (as meant by its representation in Chart 1) only in the case of the phosphinidene complex **4**, whereas there is significant delocalization over the Mo−P−Mo chain in the cases of **1** and **3**.[11a,12] Yet, the reactivity of the latter two species also seems to be focused on their short Mo−P bonds. Thus, the less congested cyclopentadienylidene−phosphinidene complex **3** has been shown to add a variety of molecules (HCl, alkynes)[13,14] and metal fragments ($Fe(CO)_4$, $Mo(CO)_5$, $Co_2(CO)_6$) across that Mo−P bond,[12,13] whereas the most congested arylphosphinidene complex **1** can only bind small metal fragments at that position, such as CuCl.[11b] It should be noted, however, that there is considerable electron density also at the metal sites in both cases, and this might enable the direct addition of an electrophile to one of the metal atoms, as actually observed in the protonation of **1**.[11]

In a preliminary investigation, we found that compounds **1** and **3** readily reacted with [AuCl(THT)] by adding a AuCl fragment to their short Mo−P bonds. Incorporation of the gold atom triggered a spontaneous isomerization of the arylphosphinidene derivative into its cyclopentadienylidene−phosphinidene isomer (a complex process requiring the cleavage and formation of different P−C and C−H bonds), thus mimicking the proton-catalyzed isomerization of **1** into **3**. Moreover, the chloride ligand could be easily removed from these products, this in turn triggering an unusual condensation involving the formation of new Mo−Au and Au−Au bonds to give a cationic Mo_4Au_2 cluster.[15] We then decided to explore the potential of these complexes in the synthesis of heterometallic gold derivatives by studying in more detail the reactions of compounds **1** and **3** with different gold(I) complexes, which we have also extended to the less congested phosphinidene complexes **2** and **4**. Some attempts to obtain related silver(I), copper(I), and mercury(II) species were also made. As will be shown below, these reactions enabled us to build up a variety of heterometallic derivatives having trinuclear Mo_2Au, tetranuclear Mo_3Au, and pentanuclear Mo_4M (M = Au, Ag, Cu) metal cores held by tricentric interactions resulting from the addition of the metallic electrophile to the multiple Mo−P bond of the parent phosphinidene substrate. In contrast, oxidative addition across that bond, or formation of Mo→M dative bonds, was observed in the reactions with HgI_2.

Chart 2

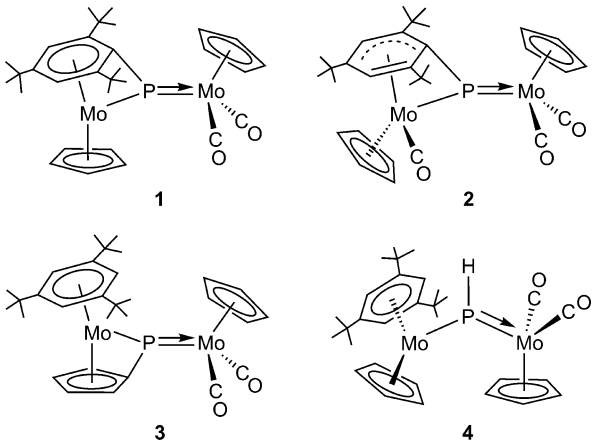

RESULTS AND DISCUSSION

Neutral AuCl Derivatives. Compounds **1** to **4** reacted readily with [AuCl(THT)] by displacing the THT ligand from the latter, to give the corresponding derivatives $[AuMo_2ClCp_2(\mu\text{-}\kappa^1{:}\kappa^1{:}\kappa^1,\eta^6\text{-PR*})(CO)_2]$ (**5**), $[AuMo_2ClCp_2(\mu\text{-}\kappa^1{:}\kappa^1{:}\kappa^1,\eta^4\text{-PR*})(CO)_3]$ (**6**), $[AuMo_2ClCp(\mu\text{-}\kappa^1{:}\kappa^1{:}\kappa^1,\eta^5\text{-}PC_5H_4)(CO)_2(\eta^6\text{-HR*})]$ (**7**), and $[AuMo_2ClCp_2(\mu_3\text{-PH})(CO)_2(\eta^6\text{-HR*})]$ (**8**). The latter complexes formally result from the addition of an acceptor AuCl moiety to the short Mo−P bond of the parent substrates almost perpendicular to the corresponding Mo_2P plane, as expected for a donor−acceptor interaction where the donor is the π(Mo−P) bonding electron pair of the phosphinidene complex (Chart 3). The phosphinidene complex **4** was the fastest substrate in this reaction (completed in a few minutes even at 213 K), as expected by considering that it displays the largest concentration of π electron density at its short Mo−P bond and the smallest steric crowding in this region of the molecule. On the other hand, the red compound **5** was found to be thermally unstable in solution, since it slowly rearranges at room

Chart 3

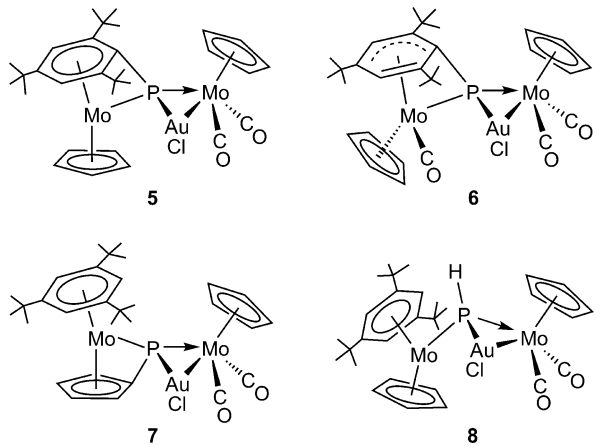

dx.doi.org/10.1021/ic501376v | Inorg. Chem. 2014, 53, 10325−10339

temperature to yield its violet cyclopentadienylidene−phosphinidene isomer **7**, a transformation that can be completed in only 10 min upon heating the crude product at 313 K in 1,2-dichloroethane. The latter complex, in turn, displays two interconverting isomers in solution, to be discussed below.

We have shown previously that the addition of CuCl to **1** gives a product analogous to **5** that reacts with CO much more easily than the parent complex **1**, to give a product analogous to **6** (see Figure 1, Table 1). A separated experiment indicated

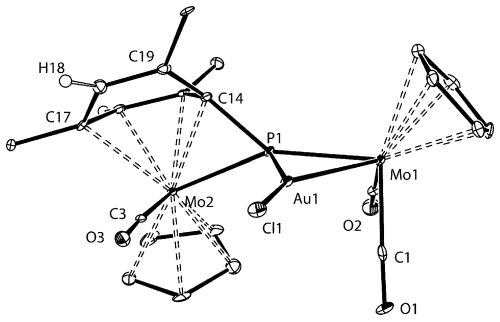

Figure 1. ORTEP diagram (30% probability) of compound **6** with H atoms (except those in the aryl ring) and ^{t}Bu groups (except their C^{1} atoms) omitted for clarity.

Table 1. Selected Bond Lengths (Å) and Angles (deg) for Compound 6

Mo1−Au1	2.8493(6)	Mo1−P1−Mo2	150.4(1)
Mo1−P1	2.306(2)	Mo1−P1−C14	143.2(2)
Mo1−C1	1.914(7)	Mo2−P1−C14	64.4(2)
Mo1−C2	2.031(8)	Mo1−P1−Au1	74.07(5)
Au1−P1	2.422(2)	Mo1−Au1−P1	51.09(4)
Au1−Cl1	2.426(2)	Mo1−Au1−Cl1	150.39(4)
Mo2−P1	2.385(2)	P1−Au1−Cl1	158.42(5)
Mo2−C3	2.111(8)	P1−Mo1−Au1	54.84(4)
Mo2−C14	2.259(6)	P1−Mo1−C1	95.8(2)
P1−C14	1.717(6)	P1−Mo1−C2	84.4(2)
C18−C19	1.338(9)	C1−Mo1−C2	82.3(3)
		P1−Mo2−C3	86.8(2)

that the presence of the AuCl fragment has the same effect on **5**, which readily adds CO (1 atm, room temperature, toluene solution), this forcing a ring slippage of the aryl ring into an η^4-coordination mode then yielding **6**, a transformation that can be rapidly reversed upon photolysis of the latter complex.

The structure of **6** in the crystal can be derived from that of the parent compound **2** by adding a AuCl moiety to the short Mo−P bond nearly perpendicular to the Mo_2P plane and from the same side as the metallocene-bound carbonyl, which is the less congested side of the molecule. The structure thus is broadly comparable to that of the CuCl derivative of **2** previously determined by us,[11b] with one important difference: in **6**, the MoPAu plane is nearly orthogonal to the Mo_2P plane, and there is no residual interaction with the carbonyls of the $MoCp(CO)_2$ fragment. In contrast, the Cu analogue of **6** has its CuCl fragment tilted so that the Cu atom approaches the C atom of a carbonyl ligand, thus effectively increasing its coordination number. These differences are expected by considering the known coordination trends of Au and Cu complexes.[16] As for the interatomic lengths within the AuMoP ring, we note that the Mo−P distance of 2.306(2) Å is somewhat longer than the values of ca. 2.25 Å in the Mo_2 precursors but still quite short for a single bond (expected above ca. 2.40 Å). On the other hand, the Au−Mo (2.8493(6) Å) and Au−P (2.422(2) Å) lengths are a bit longer than the reference single-bond distances (cf. 2.710(1) Å in $[MoAuCp(CO)_3(PPh_3)]$[17] and 2.309(2) Å in $[Mo_2AuCp_2(\mu_3\text{-}PH)(CO)_4(PPh_3)]$).[8] All of these structural features are consistent with our description of the bonding in compounds **5** to **8** as donor/acceptor interactions resulting in tricentric AuMoP bonds. In line with this interpretation, the intermetallic length in **6** is close to the average Mo−Au length of ca. 2.88 Å determined for $[Mo_2AuCp_2(\mu\text{-}PPh_2)(CO)_4(PPh_3)]$, a cluster displaying a triangular Mo_2Au central core.[18] We finally note that the Au−Cl length of 2.426(2) Å is unexpectedly large when compared to those usually encountered in mononuclear $[AuCl(PR_3)]$ complexes (usually in the range 2.27−2.31 Å, according to a search in the CCDC database), or even when compared to that in the phosphinidene-bridged complex $[AuFe_2ClCp_2(\mu\text{-}PCy)(\mu\text{-}CO)(CO)_2]$ (2.315(1) Å).[8] Actually, such large Au−Cl separations have only been found previously in several heterobimetallic Au(II) complexes displaying square planar $MClP_2$ environments around the gold atoms.[19] All of this suggests that the mentioned donor/acceptor interaction involved in the formation of compounds **5** to **8** is particularly strong, so as to weaken the Au−Cl bond significantly, in agreement with the chemistry of these trinuclear complexes, to be briefly discussed below.

Spectroscopic data in solution for compounds **5** to **8** (Table 2 and Experimental Section) are consistent with structures analogous to the one discussed for **6**. All these compounds display ^{31}P NMR resonances in the range 350−400 ppm, some 110−140 ppm more shielded than those of the corresponding parent compounds, in agreement with the change in coordination mode (from trigonal μ_2-PR to μ_3-PR) operated on the phosphinidene ligand.[20] Their IR spectra display C−O stretching bands with intensities (very strong and strong, in order of decreasing frequencies) indicative of the presence of cisoid $Mo(CO)_2$ oscillators defining angles somewhat below 90°,[21] in agreement with the angle of 82.3(3)° found for **6** in the crystal. As expected, compound **6** displays an additional band (1974 cm^{-1}) due to the carbonyl bound to the metallocene fragment. The average frequencies of the $M(CO)_2$ oscillators in these compounds are some 40−45 cm^{-1} higher than the figures in the corresponding parent compounds, this reflecting the strong acceptor role of the AuCl fragment in these molecules. Moreover, the presence of the latter fragment sideways from the original Mo_2P plane removes any symmetry plane present in the parent compounds, which is reflected in the full inequivalence of the C and H atoms of the aryl or C_5H_4 rings in compounds **5** and **7**. We finally note that the PH ligand in compound **8** gives rise to a strongly deshielded ^{1}H NMR resonance at 9.06 ppm displaying a relatively low P−H coupling of 238 Hz, as found for the $M(CO)_n$ derivatives of compound **4** (with couplings around 220 Hz), a feature that we have identified as an indirect effect of the absence of intermetallic bonding in this sort of trinuclear species.[12]

As noted above, compound **7** displays in solution two interconverting isomers with similar spectroscopic properties, likely differing in the relative orientation of the C_5 rings with respect to the MoPAu plane (*syn* and *anti*, Chart 4). This isomerism has been previously found (both in solution and in the solid state) for the chalcogenophosphinidene derivatives of **2** and **3**, which are structurally related to compounds **7**, with the *anti* isomers being only slightly more favored in solution,

dx.doi.org/10.1021/ic501376v | *Inorg. Chem.* 2014, 53, 10325−10339

Table 2. Selected IR[a] and $^{31}P\{^1H\}$ NMR Data[b] for New Compounds

compound	ν(CO)	δ_P (J_{PP})
$[AuMo_2ClCp_2(\mu\text{-}\kappa^1\text{:}\kappa^1\text{:}\kappa^1,\eta^6\text{-PR*})(CO)_2]$ (**5**)	1932 (vs), 1864 (s)	400.2
$[AuMo_2ClCp_2(\mu\text{-}\kappa^1\text{:}\kappa^1\text{:}\kappa^1,\eta^4\text{-PR*})(CO)_3]$ (**6**)	1974 (m), 1941 (vs), 1869 (s)	356.0
$[AuMo_2ClCp(\mu\text{-}\kappa^1\text{:}\kappa^1\text{:}\kappa^1,\eta^5\text{-}PC_5H_4)(CO)_2(\eta^6\text{-HR*})]$ (**7**)	1942 (vs), 1870 (s)	380.2 (*anti*), 388.1 (*syn*)[c]
$[AuMo_2ClCp_2(\mu_3\text{-PH})(CO)_2(\eta^6\text{-HR*})]$ (**8**)	1924 (vs), 1847 (s)	357.7
$[AuMo_3Cp_2(\mu\text{-}\kappa^1\text{:}\kappa^1\text{:}\kappa^1,\eta^5\text{-}PC_5H_4)(CO)_5(\eta^6\text{-HR*})]$ (**9**)	1942 (m, sh), 1927 (vs), 1855 (s), 1831 (m)	387.2 (*anti*), 404.0 (*syn*)[c]
$[HgMo_2Cp_2(\mu\text{-I})I(\mu\text{-}\kappa^1\text{:}\kappa^1,\eta^6\text{-PR*})(CO)_2]_2$ (**10**)	1940 (m), 1884 (vs)	640.3[d]
$[HgMo_2CpI_2(\mu\text{-}\kappa^1\text{:}\kappa^1,\eta^5\text{-}PC_5H_4)(CO)_2(\eta^6\text{-HR*})]$ (**11**)	1943 (vs), 1862 (s)	32.0[e]
$[AuMo_2Cp_2(\mu\text{-}\kappa^1\text{:}\kappa^1,\eta^6\text{-PR*})(CO)_2(THT)](PF_6)$ (**12a**)	1937 (vs), 1869 (s)	420.0
$[AuMo_2Cp_2(\mu\text{-}\kappa^1\text{:}\kappa^1,\eta^6\text{-PR*})(CO)_2\{P(p\text{-tol})_3\}](PF_6)$ (**12b**)	1936 (vs), 1868 (s)	449 (br), 50.3 (d, 42)
$[AuMo_2Cp_2(\mu\text{-}\kappa^1\text{:}\kappa^1,\eta^6\text{-PR*})(CO)_2(PMe_3)](PF_6)$ (**12c**)	1933 (vs), 1867 (s)	429.1 (br), 13.7 (d, 57)
$[AuMo_2Cp_2(\mu\text{-}\kappa^1\text{:}\kappa^1\text{:}\kappa^1,\eta^4\text{-PR*})(CO)_3(THT)](PF_6)$ (**13a**)	1957 (m, sh), 1945 (vs), 1880 (m)	402.4
$[AuMo_2Cp_2(\mu\text{-}\kappa^1\text{:}\kappa^1\text{:}\kappa^1,\eta^4\text{-PR*})(CO)_3\{P(p\text{-tol})_3\}](PF_6)$ (**13b**)	1962 (m, sh), 1943 (vs), 1876 (s)	420.8 (d, 59), 57.2 (d, 59)
$[AuMo_2Cp(\mu\text{-}\kappa^1\text{:}\kappa^1\text{:}\kappa^1,\eta^5\text{-}PC_5H_4)(CO)_2(\eta^6\text{-HR*})\{P(p\text{-tol})_3\}](PF_6)$ (**14b**)	1943 (vs), 1875 (s)	451.4 (d, 55), 60.6(d, 55)
$[AuMo_2Cp_2(\mu_3\text{-PH})(CO)_2(\eta^6\text{-HR*})\{P(p\text{-tol})_3\}](BAr'_4)$ (**15b**)	1929 (vs), 1856 (s)	425.0 (d, 65), 60.4 (d, 65)
$[AuMo_2Cp_2(\mu_3\text{-PH})(CO)_2(\eta^6\text{-HR*})(PMe_3)](BAr'_4)$ (**15c**)	1927 (vs), 1854 (s)	416.6 (d, 68), 30.7 (d, 68)
$[AuMo_2Cp_2(\mu_3\text{-PH})(CO)_2(\eta^6\text{-HR*})(P^iPr_3)](BAr'_4)$ (**15d**)	1928 (vs), 1855 (s)	422.7 (d, 60), 92.2 (d, 60)
$[Au\{Mo_2Cp_2(\mu\text{-}\kappa^1\text{:}\kappa^1\text{:}\kappa^1,\eta^6\text{-PR*})(CO)_2\}_2](PF_6)$ (**16**)	1932 (vs), 1863 (s)	435.6
$[Au\{Mo_2Cp(\mu\text{-}\kappa^1\text{:}\kappa^1\text{:}\kappa^1,\eta^5\text{-}PC_5H_4)(CO)_2(\eta^6\text{-HR*})\}_2](PF_6)$ (**17**)	1938 (vs), 1869 (s)	440.1
$[Au\{Mo_2Cp_2(\mu_3\text{-PH})(CO)_2(\eta^6\text{-HR*})\}_2](BAr'_4)$ (**18**)	1937 (m, sh), 1916 (vs), 1849 (s)[f]	434–417[f]
$[Ag\{Mo_2Cp(\mu\text{-}\kappa^1\text{:}\kappa^1\text{:}\kappa^1,\eta^5\text{-}PC_5H_4)(CO)_2(\eta^6\text{-HR*})\}_2](PF_6)$ (**19**)	1934 (vs), 1863 (s)	468.0
$[Ag\{Mo_2Cp(\mu\text{-}\kappa^1\text{:}\kappa^1\text{:}\kappa^1,\eta^5\text{-}PC_5H_4)(CO)_2(\eta^6\text{-HR*})\}_2]$ (BAr'_4) (**19′**)	1934 (vs), 1864 (s)	468.0 (d, br)[g]
$[Ag\{Mo_2Cp_2(\mu_3\text{-PH})(CO)_2(\eta^6\text{-HR*})\}_2](BAr'_4)$ (**20**)	1912 (vs), 1840 (s)	474.4 (d, br)[h]
$[Cu\{Mo_2Cp_2(\mu\text{-}\kappa^1\text{:}\kappa^1\text{:}\kappa^1,\eta^6\text{-PR*})(CO)_2\}_2](PF_6)$ (**21**)	1918 (vs), 1844 (s)	420.9

[a]Recorded in dichloromethane solution, with C–O stretching bands [ν(CO)] in cm^{-1}; R* = 2,4,6-$C_6H_2{}^tBu_3$; THT = SC_4H_8; Ar′ = 3,5-$C_6H_3(CF_3)_2$. [b]Recorded in CD_2Cl_2 at 121.50 MHz and 295 K, J_{PP} in Hz; all PF_6^- salts also displayed a septet resonance at ca. −145 ppm (J_{PF} = 710 Hz) due to this anion. [c]Minor isomer (see text). [d]$J(^{31}P-^{199}Hg)$ = 536 Hz. [e]$J(^{31}P-^{199}Hg)$ = 1604 Hz. [f]Four isomers are present in solution, with resonances at 433.8, 427.6, 423.6, and 417.4 ppm in a ratio of ca. 1:6:4:1, respectively (see the Experimental Section). [g]$J(^{31}P-^{109}Ag) \approx J(^{31}P-^{107}Ag) \approx 90$ Hz. [h]$J^{109}_{AgP} \approx J^{107}_{AgP}$ = 100 Hz.

presumably on steric grounds.[22] Accordingly, we identify the major isomer of **7** in solution as the corresponding *anti* isomer. The interconversion between *syn* and *anti* isomers would likely occur as proposed for the chalcogenophosphinidene derivatives of **3**, that is, via a transitory cleavage of the P–$MoCp(CO)_2$ bond,[22] which in the current case would allow for the rotation of the $MoCp(CO)_2$ fragment around the Mo–Au bond.

Chart 4

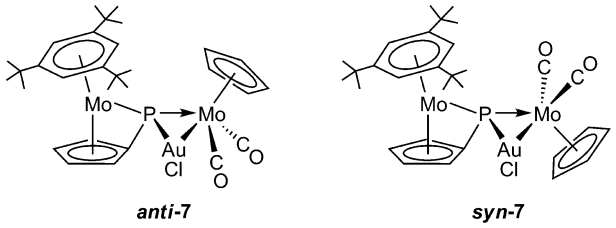

Synthesis and Characterization of the Tetranuclear Derivative 9. In our preliminary study on this chemistry, we noticed that removal of the chloride ligand from compounds **5** and **7** eventually induced self-assembly of the cation to give an unusual Mo_4Au_2 cluster.[15] We have now checked the potential of the AuCl derivatives of compounds **1**–**4** as synthetic precursors of novel heterotrimetallic derivatives by examining the reaction of **7** with a simple metal carbonylate such as $K[MoCp(CO)_3]$. Indeed, this reaction takes place rapidly at 213 K to give the expected tetranuclear complex $[AuMo_3Cp_2(\mu\text{-}\kappa^1\text{:}\kappa^1\text{:}\kappa^1,\eta^5\text{-}PC_5H_4)(CO)_5(\eta^6\text{-HR*})]$ (**9**) following from nucleophilic substitution of the gold-bound chloride ligand with the molybdenum carbonylate, thus generating a new Au–Mo bond (Scheme 1).

Scheme 1

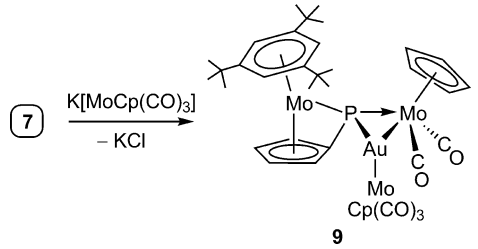

The structure of **9** in the crystal expectedly displays a $MoCp(CO)_3$ fragment replacing the chloride ligand of the parent compound **7** (Figure 2 and Table 3). Incidentally, we note that there are three independent molecules in the unit cell, but otherwise similar to each other, so that only selected parameters for one of them have been collected in Table 3 and

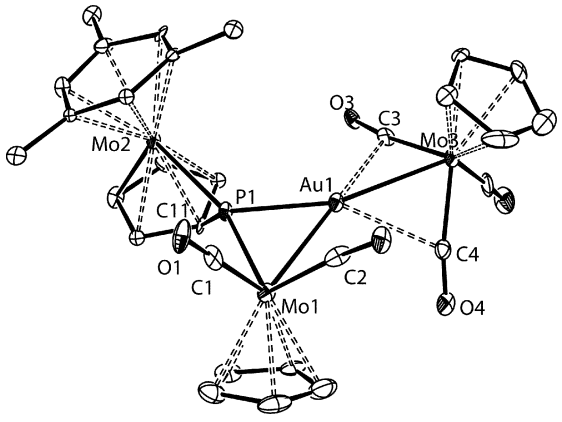

Figure 2. ORTEP diagram (30% probability) of compound **9** with H atoms and ^tBu groups (except their C^1 atoms) omitted for clarity. Only one of the three independent molecules present in the unit cell is shown.

dx.doi.org/10.1021/ic501376v | Inorg. Chem. 2014, 53, 10325–10339

Table 3. Selected Bond Lengths (Å) and Angles (deg) for Compound 9

Mo1−Au1	2.807(2)	C1−Mo1−C2	79.4(7)
Mo1−P1	2.344(4)	P1−Mo1−C1	88.5(5)
Mo2−P1	2.431(4)	P1−Mo1−C2	109.3(5)
Au1−Mo3	2.711(2)	P1−Mo1−Au1	53.5(1)
Au1−P1	2.353(4)	P1−Au1−Mo1	53.2(1)
P1−C11	1.80(2)	Mo1−P1−Au1	73.4(1)
Mo1−C1	1.95(2)	C3−Mo3−C4	104.1(6)
Mo1−C2	1.98(2)	Au1−Mo3−C5	118.2(5)
Mo3−C3	1.95(2)	C3−Mo3−C5	80.0(7)
Mo3−C4	1.97(2)	C4−Mo3−C5	80.9(7)
Mo3−C5	1.97(2)	Mo3−C3−O3	171(2)
Au1···C3	2.57(2)	Mo3−C4−O4	172(2)
Au1···C4	2.52(2)	Mo3−C5−O5	177(2)

are discussed below. The newly formed Mo−Au bond now corresponds formally to a bicentric interaction, and accordingly, the corresponding distance of 2.711(2) Å is essentially identical to those measured for the binuclear complexes $[AuMo(C_5H_4R)(CO)_2(PPh_3)]$ (R = H,[17] $C_2H_4NMe_2$)[23] or the trinuclear anion $[Mo_2AuCp_2(CO)_6]^-$.[24] As for the MoAuP ring, the Mo−Au and P−Au lengths are ca. 0.05−0.07 Å shorter than the corresponding lengths in **6**, whereas the P1−Mo1 length is longer, which suggests that the tricentric interaction within this ring is stronger for **9**. We finally note the presence of weak semibridging interactions between the gold atom and the cisoid carbonyls of the carbonylate fragment (Au···C ca. 2.55 Å, Mo−C−O ca. 172°). Similar interactions are present in the MoAu complexes mentioned above[17,23,24] and are common in heterometallic carbonyl clusters containing gold atoms,[4b] although it is doubtful whether they are of genuinely bonding nature.

In solution, compound **9** displays two interconverting isomers in a ratio (ca. 1/5 in toluene-d_8) similar to that found for the parent compound **7**, with the major isomer giving rise also to the more shielded ^{31}P NMR resonance and being analogously identified as the one derived from the *anti* isomer of **7** (note that the crystal contains a derivative of the minor, *syn* isomer of **7**). Even if the newly incorporated $MoCp(CO)_3$ fragment might adopt different conformations in solution relative to the original Mo_2P fragment, it is likely that these interconvert rapidly through rotation around the newly formed Mo−Au bond and do not give rise to observable isomerism. Actually, the room temperature ^{13}C NMR spectrum of **9** displays a single resonance at 231.4 ppm for all carbonyls of the $MoCp(CO)_3$ fragment, consistent with this dynamic behavior. Although we have not recorded low temperature ^{13}C NMR spectra of this complex, we trust that the weak semibridging interactions present in the crystal lattice probably are retained in solution, since the IR spectrum of **9** lacks the strong high-frequency C−O stretching band above 2000 cm^{-1} characteristic of $MoCp(CO)_3$ fragments,[21] while it displays a band at somewhat low frequency (1831 cm^{-1}) as expected for semibridging carbonyls, in addition to the bands attributable to the $MoCp(CO)_2$ oscillator of the molecule (1927, 1855 cm^{-1}, Table 2).

Neutral HgI_2 Derivatives. Compound **1** reacts with HgI_2 to give the red-brick complex $[HgMo_2Cp_2(\mu\text{-}I)I(\mu\text{-}\kappa^1\text{:}\kappa^1,\eta^6\text{-}PR^*)(CO)_2]_2$ (**10**), a stable substance retaining a μ_2-PR ligand that we could isolate properly and fully characterize. In contrast, the PC_5H_4 complex **3** reacted with HgI_2 to give a yellow-brown derivative of analogous composition but different spectroscopic properties, tentatively identified as the μ_3-PR bridged complex $[HgMo_2CpI_2(\mu\text{-}\kappa^1\text{:}\kappa^1\text{:}\kappa^1,\eta^5\text{-}PC_5H_4)(CO)_2(\eta^6\text{-}HR^*)]$ (**11**; Chart 5). Compound **11** could not be isolated as a pure

Chart 5

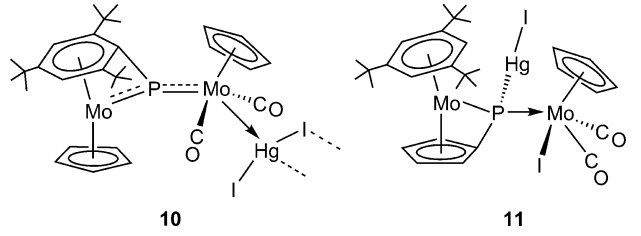

10 **11**

substance since it progressively hydrolyzes to give the phosphide-bridged complex $[Mo_2Cp\{\mu\text{-}\kappa^1\text{:}\kappa^1,\eta^5\text{-}P(H)C_5H_4\}(I)(CO)_2(\eta^6\text{-}R^*H)]$, a substance comparable to the chloro complex following from the addition of HCl to the short Mo−P bond in **3**.[13] Indeed, the structure proposed for **11** is one following from the addition of a Hg−I bond to the same Mo−P bond in **3**, with specific formation of new P−Hg and Mo−I bonds.

The hexanuclear molecule of **10** in the solid state (Figure 3 and Table 4) can be viewed as derived from a donor/acceptor

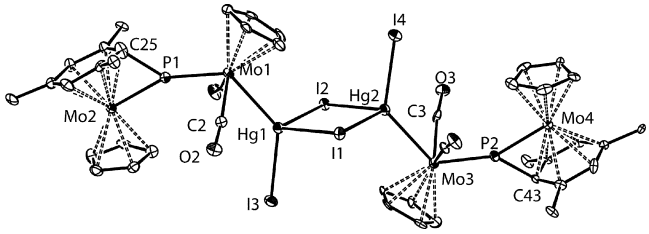

Figure 3. ORTEP diagram (30% probability) of compound **10** with H atoms and ^{t}Bu groups (except their C^1 atoms) omitted for clarity.

interaction between **1** (the donor) and HgI_2 (acceptor) resulting in the formation of a dative Mo→Hg bond[25] and further dimerization of the resulting adduct via formation of Hg−I−Hg bridges, thus achieving a tetrahedral environment around the Hg atoms comparable to that in the phosphine

Table 4. Selected Bond Lengths (Å) and Angles (deg) for Compound 10

Mo1−P1	2.294(3)	Mo3−P2	2.288(3)
Mo2−P1	2.301(3)	Mo4−P2	2.302(3)
Mo1−Hg1	2.820(1)	Mo3−Hg2	2.827(1)
Mo1−C1	1.98(1)	Mo3−C3	2.00(1)
Mo1−C2	1.99(1)	Mo3−C4	1.94(2)
Hg1−I1	3.091(1)	Hg2−I1	2.894(1)
Hg1−I2	2.914(1)	Hg2−I2	3.070(1)
Hg1−I3	2.765(1)	Hg2−I4	2.776(1)
P1−C25	1.86(2)	P2−C43	1.85(1)
Mo1−P1−Mo2	153.1(2)	Mo1−Hg1−I3	132.91(3)
Mo1−P1−C25	143.7(5)	Mo1−Hg1−I2	113.36(3)
Mo2−P1−C25	63.0(5)	Mo1−Hg1−I1	106.31(3)
P1−Mo1−Hg1	126.6(1)	I1−Hg1−I2	96.71(3)
P1−Mo1−C1	79.9(4)	Hg1−I1−Hg2	82.84(2)
P1−Mo1−C2	79.2(4)	Hg1−I2−Hg2	82.86(2)
C1−Mo1−C2	100.1(5)		

dx.doi.org/10.1021/ic501376v | *Inorg. Chem.* 2014, 53, 10325−10339

adducts of mercury(II) halides $[Hg_2(\mu\text{-}X)_2X_2(PR_3)_2]$. The average terminal and bridging I–Hg lengths in **10** (2.77 and 2.99 Å) are ca. 0.1 Å longer than the corresponding values in $[Hg_2(\mu\text{-}I)_2I_2(PPh_3)_2]$ (2.68 and 2.92 Å, respectively),[26] which suggests a very efficient electron donation from the molybdenum atom to the mercury center. The corresponding Mo–Hg lengths of ca. 2.82 Å in **10** are only a bit longer than the value of 2.745 Å measured for $[HgMoCl_2(\eta^6\text{-}C_6H_3Me_3)(CO)_3]$,[27] which stands as the only other complex with a dative Mo→Hg bond structurally characterized to date, and are still shorter than the sum of covalent radii for these atoms (2.86 Å).[28] Yet these lengths are significantly longer than those measured in related species containing "normal" Mo–Hg(II) bonds, such as the complexes $[MoL(CO)_3(HgX)]$ (ca. 2.68 Å; X = Cl, L = Cp, C_5H_4Me; X = I, L = $C_5H_3Ph_2$).[29]

The overall geometry of the dimolybdenum fragment in **10** is modestly perturbed with respect to the parent compound **1**, this involving some rearrangement in the $MoCp(CO)_2$ moiety to accommodate the mercury atom *trans* to the phosphinidene ligand (Hg–Mo–P ca. 126°; OC–Mo–CO ca. 100°). We therefore conclude that adduct formation occurs via a metal-based nonbonding electron pair of **1**, as observed in the protonation of the latter to give initially a hydride intermediate having a transoid $MoCp(CO)_2H(PR)$ moiety.[11a] As a result of this acid/base interaction, both the trigonal environment around the P atom and the symmetry plane bisecting the aryl ligands are preserved. Interestingly, the Mo–P lengths now are almost identical to each other and short, with a value of ca. 2.30 Å comparable to the average figure of 2.31 Å for the type **A** complex $[Mo_2Cp_2(\mu\text{-}PR^*)(CO)_4]$.[30] Thus, we conclude that electron redistribution in **1** upon adduct formation with HgI_2 results in full delocalization of the π(P–Mo) interaction along the Mo–P–Mo chain to yield effective bond orders of 1.5.

Spectroscopic data in solution for **10** are consistent with the structure found in the crystal. In particular, the pattern of the C–O stretches (medium and very strong, in order of decreasing frequencies) are characteristic of transoid $M(CO)_2$ oscillators with C–M–C angles above 90° (ca. 100° in the crystal), and its ^{1}H NMR spectrum denotes the presence of a symmetry plane bisecting the aryl group of the phosphinidene ligand. The latter in turn gives rise to a ^{31}P NMR resonance at 640.3 ppm, ca. 130 ppm more deshielded than that of **1** (opposite behavior to that observed upon formation of compounds **5** to **8**), in agreement with retention of the trigonal environment around the P atom and π(Mo–P–Mo) bonding (cf. 685.6 ppm for $[Mo_2Cp_2(\mu\text{-}PR^*)(CO)_4]$).[30] The coupling of 536 Hz to the ^{199}Hg nucleus is significantly higher than the values measured for phosphine complexes of the type *trans*-$[MoCp(CO)_2(PR_3)(HgX)]$ (ca. 360–460 Hz),[31] an effect possibly related to the mentioned multiplicity of the Mo–P bond in **10**.

The nature of **10** can be in part understood by taking into account the severe crowding around the short Mo–P bond in **1** that would disfavor any reaction from taking place at that point, moreover it also illustrates the first step in the reaction of **1** with H^+, as noted above. This crowding is less severe in **3**, which indeed is able to add $M(CO)_5$ and $M(CO)_4$ metal fragments at its short Mo–P bond to give stable heterometallic derivatives.[12] Thus, perhaps it is not surprising that **3** reacts with HgI_2 to give **11**, a complex derived from the addition of a Hg–I bond to the short Mo–P bond of **3**. In agreement with this, the IR spectrum of **11** denotes the presence of a cisoid $Mo(CO)_2$ fragment in the molecule. Moreover its ^{31}P NMR spectrum displays a strongly shielded resonance (δ_P 32.0 ppm), in a position comparable to that of the phosphide-bridged complex $[Mo_2Cp\{\mu\text{-}\kappa^1\text{:}\kappa^1,\eta^5\text{-}P(H)C_5H_4\}(Cl)(CO)_2(\eta^6\text{-}R^*H)]$ (ca. −14 ppm),[13] while the large coupling of 1604 Hz is consistent with direct binding of the phosphinidene ligand to the mercury atom.[32] We finally note that, since both the P atom and the $Mo(CO)_2$ center of **11** are stereogenic centers, two different diastereoisomers are possible for this trinuclear complex, but apparently only one is formed, which we have tentatively formulated as the one emerging from a transoid addition of HgI_2 to the double Mo–P bond of **3** (Chart 5).

Cationic AuL Derivatives. Compounds **1**–**3** react readily with stoichiometric amounts of the THT adducts $[AuL(THT)]PF_6$ to give the corresponding trinuclear derivatives **12**–**14** resulting from the addition of a AuL^+ fragment to the short Mo–P bond of the parent substrates: the red complexes $[AuMo_2Cp_2(\mu\text{-}\kappa^1\text{:}\kappa^1\text{:}\kappa^1,\eta^6\text{-}PR^*)(CO)_2L](PF_6)$ [L = THT (**12a**), P(*p*-tol)$_3$ (**12b**), PMe_3 (**12c**)] and $[AuMo_2Cp_2(\mu\text{-}\kappa^1\text{:}\kappa^1\text{:}\kappa^1,\eta^4\text{-}PR^*)(CO)_3L](PF_6)$ [L = THT (**13a**), P(*p*-tol)$_3$ (**13b**)] and the green complex $[AuMo_2Cp(\mu\text{-}\kappa^1\text{:}\kappa^1\text{:}\kappa^1,\eta^5\text{-}PC_5H_4)(CO)_2(\eta^6\text{-}HR^*)\{P(p\text{-tol})_3\}](PF_6)$ (**14b**; Chart 6).

Chart 6

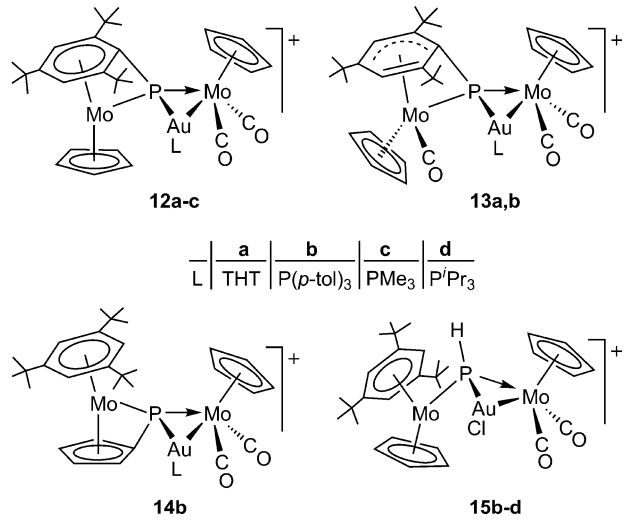

The blue, analogous derivatives of **4** were more conveniently isolated as tetraarylborate salts $[AuMo_2Cp_2(\mu_3\text{-}PH)(CO)_2(\eta^6\text{-}HR^*)L](BAr'_4)$ [L = P(*p*-tol)$_3$ (**15b**), PMe_3 (**15c**), P^{i}Pr$_3$ (**15d**); Ar′ = 3,5-$C_6H_3(CF_3)_2$]. The stability of these cations was not the same in all cases, and some of these compounds underwent spontaneous symmetrization at room temperature to give pentanuclear derivatives by following eq 1 (Mo_2 represents the parent substrates **1** to **4**). This was the case, for instance, of the PC_5H_4-bridged compound **14b**, which slowly undergoes symmetrization in solution at room temperature, while the analogous PMe_3 complex could not be even detected in the reaction of **3** with $[Au(PMe_3)(THT)]PF_6$, this instead leading directly to the same pentanuclear Mo_4Au derivative. This sort of reaction is not uncommon in the chemistry of heterometallic gold complexes.[4b]

$$2[Mo_2AuL]^+ \rightarrow [Mo_4Au]^+ + [AuL_2]^+ \quad (1)$$

Analogous symmetrization processes also occurred spontaneously upon attempted preparation of related trinuclear silver complexes through reactions of **3** or **4** with the cation

dx.doi.org/10.1021/ic501376v | Inorg. Chem. 2014, 53, 10325–10339

$[Ag(PPh_3)(THT)]^+$, which gave instead pentanuclear Mo_4Ag derivatives and $[Ag(PPh_3)_2]^+$, as discussed below.

The structure of the THT adduct **12a** was determined in our preliminary study on this chemistry.[15] We have now determined the structures of the gold-phosphine derivatives **13b** (PR*-bridged, Figure 4) and **15d** (PH-bridged, Figure 5),

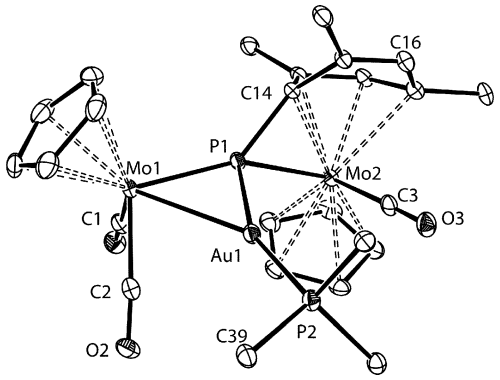

Figure 4. ORTEP diagram (30% probability) of the cation in compound **13b** with H atoms, *p*-tol, and ^{t}Bu groups (except their C^1 atoms) omitted for clarity.

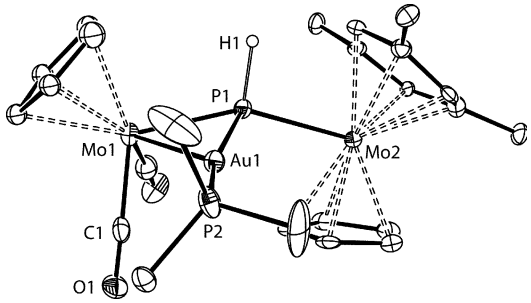

Figure 5. ORTEP diagram (30% probability) of the cation in compound **15d** with H atoms (except H1) and ^{t}Bu and ^{i}Pr groups (except their C^1 atoms) omitted for clarity.

with the most relevant geometrical parameters being collected in Tables 5 and 6. The structure of the tricarbonyl complex **13b**

Table 5. Selected Bond Lengths (Å) and Angles (deg) for Compound 13b

Mo1−P1	2.313(1)	Mo1−P1−Mo2	153.47(4)
Mo2−P1	2.368(1)	Mo1−P1−C14	140.0(1)
Mo1−Au1	2.8080(3)	Mo2−P1−C14	65.0(1)
Mo1−C1	1.962(4)	C1−Mo1−C2	79.2(2)
Mo1−C2	1.987(4)	P1−Mo1−C1	85.4(1)
Mo2−C3	2.011(4)	P1−Mo1−C2	106.0(1)
Mo2−C14	2.289(4)	P1−Mo2−C3	91.6(1)
Au1−P1	2.431(1)	Mo1−P1−Au1	72.55(3)
Au1−P2	2.314(1)	P1−Mo1−Au1	55.67(2)
P1−C14	1.794(3)	Mo1−Au1−P2	149.54(2)
		P1−Au1−P2	158.66(3)

is completely analogous to that of **12a** and to that of the AuCl adduct **6** discussed above, if we just replace the chloride with a phosphine ligand at the gold atom (Au1−P2 = 2.314(1) Å). In spite of their different overall charges (neutral vs cationic), the interatomic lengths at the central Mo_2PAu core in these two

Table 6. Selected Bond Lengths (Å) and Angles (deg) for Compound 15d

Mo1−P1	2.360(2)	Mo1−P1−Mo2	146.8(1)
Mo2−P1	2.510(2)	Mo1−P1−H1	110(3)
Mo1−Au1	2.8038(6)	Mo2−P1−H1	100(3)
Mo1−C1	1.959(9)	C1−Mo1−C2	78.5(3)
Mo1−C2	1.929(9)	P1−Mo1−C1	107.0(2)
Au1−P1	2.421(2)	P1−Mo1−C2	87.4(3)
Au1−P2	2.313(2)	Mo1−P1−Au1	71.8(1)
P1−H1	1.45(6)	P1−Mo1−Au1	55.1(1)
		Mo1−Au1−P2	139.8(1)
		P1−Au1−P2	165.6(1)

complexes are comparable to each other, and no detailed discussion is required.

The structure of the PH-bridged complex **15d** also is comparable to those of compounds **6**, **12a**, and **13b** except for the Mo−P distances, which are significantly longer. Thus, the Mo1−P1 length of 2.510(2) Å in **15d** now approaches the reference values of more conventional single bonds (cf. 2.555(3) Å in $[W_2Cp_2(\mu\text{-PMes})(CO)_4(PH_2Mes)]$),[33] and the Mo2−P1 length of 2.360(2) Å is closer to values of conventional dative P→Mo bonds (ca. 2.45 Å in Mo(II) PR_3 complexes). This suggests that at least the short distances found for the P−Mo(metallocene) bonds in compounds **6**, **12a**, and **13b** might not have a genuinely electronic origin but rather result from geometrical restrictions imposed by the bifunctional nature of the phosphinidene ligands present in these molecules.

Spectroscopic data in solution for compounds **12** to **15** (Table 2 and Experimental Section) are consistent with the solid-state structures discussed above. First we note that all these compounds display two C−O stretches in the IR spectrum with the pattern characteristic of cisoid $M(CO)_2$ oscillators (C−Mo−C ca. 79° for **13b** and **15d** in the crystal). This arrangement also implies that the P−Mo−CO angles are quite different from each other (ca. 90 and 107°), thus leading to quite different P−C couplings for the corresponding ^{13}C NMR resonances (e.g., 27 and 0 Hz respectively for **15c**).[34] Of course, the tricarbonyl complexes **13** display an additional CO stretch and ^{13}C NMR resonance. Interestingly, in spite of the overall positive charge of all these complexes, the average C−O stretching frequency of their $Mo(CO)_2$ oscillators is only slightly higher than those of the corresponding neutral complexes **5** to **8**, they being some 50 cm^{-1} higher than the figures of the corresponding parent compounds, with the exception of the PC_5H_4 complex **14b** (only 41 cm^{-1} above **3**).

Compounds **12** to **15** display ^{31}P NMR resonances in the range 400−450 ppm, consistent with the presence of μ_3-PR ligands, they being some 50−65 ppm more deshielded than the resonances of the corresponding neutral AuCl complexes. In addition, the phosphine-containing complexes display a second, much more shielded resonance corresponding to the gold-bound phosphine ligands, displaying a relatively large two-bond P−P coupling of 42−68 Hz with the phosphinidene ligand, consistent with the very large P−Au−P angle in these molecules (ca. 160° for **13b** and **15d** in the crystal).[20,34a] We finally note that the PH-bridged complexes **15** display strongly deshielded ^1H NMR resonances (δ_H ca. 12 ppm) characteristic of their PH ligands, with PH couplings of ca. 230 Hz comparable to those measured in heterometallic derivatives of **4** with open Mo_2M central cores (M = Fe, Cr, Mo, W).[12]

dx.doi.org/10.1021/ic501376v | *Inorg. Chem.* 2014, 53, 10325−10339

Pentanuclear Mo_4M Derivatives. Compounds **1**, **3**, and **4** reacted readily with the cation $[Au(THT)_2]^+$ (as PF_6^- or $BAr'_4{}^-$ salts) in a 2:1 ratio to give selectively the corresponding pentanuclear derivatives $[Au\{Mo_2Cp_2(\mu\text{-}\kappa^1{:}\kappa^1{:}\kappa^1,\eta^6\text{-}PR^*)(CO)_2\}_2](PF_6)$ (**16**), $[Au\{Mo_2Cp(\mu\text{-}\kappa^1{:}\kappa^1{:}\kappa^1,\eta^5\text{-}PC_5H_4)(CO)_2(\eta^6\text{-}HR^*)\}_2](PF_6)$ (**17**), and $[Au\{Mo_2Cp_2(\mu_3\text{-}PH)(CO)_2(\eta^6\text{-}HR^*)\}_2](BAr'_4)$ (**18**), respectively (Chart 7). As noted above, the trimetal complex **14b** undergoes spontaneous symmetrization in solution at room temperature to give the corresponding pentanuclear derivative **17** and $[Au(P(p\text{-}tol_3)_2]^+$. In fact, related symmetrizations can be also induced on the trinuclear arylphosphinidene complexes **12a**–**12c** upon refluxing in 1,2-dichloroethane solution, but the product obtained is the PC_5H_4 complex **17** instead of **16**, which means that the thermal treatment promotes both the symmetrization and an aryl/cyclopentadienyl isomerization of the phosphinidene ligand as observed in the neutral AuCl adduct **5**. As expected, the arylphosphinidene complex **16** also rearranges upon heating to give the isomeric cyclopentadienylidene–phosphinidene isomer **17**, which seems to be the thermodynamic sink of all these gold complexes (Scheme 2).

Attempts to use simple silver(I) salts to build related Mo_4Ag complexes was unsuccessful and led to oxidation products. However, as noted above, reaction of compounds **3** and **4** with the phosphine complex $[Ag(PPh_3)(THT)]^+$ occurred spontaneously with full symmetrization to give $[Ag(PPh_3)_2]^+$ and the corresponding pentanuclear derivatives $[Ag\{Mo_2Cp(\mu\text{-}\kappa^1{:}\kappa^1{:}\kappa^1,\eta^5\text{-}PC_5H_4)(CO)_2(\eta^6\text{-}HR^*)\}_2](PF_6)$ (**19**) and $[Ag\{Mo_2Cp_2(\mu_3\text{-}PH)(CO)_2(\eta^6\text{-}HR^*)\}_2](BAr'_4)$ (**20**) in good yield (Chart 7). From all this, we conclude that the appropriate matching between the donor phosphinidene complex and group 11 acceptor plays a critical role in all these reactions. In line with this, we note that we could prepare the related arylphosphinidene bridged copper complex $[Cu\{Mo_2Cp_2(\mu\text{-}\kappa^1{:}\kappa^1{:}\kappa^1,\eta^6\text{-}PR^*)(CO)_2\}_2](PF_6)$ (**21**) upon reaction of **1** with $[Cu(NCMe)_4]BF_4$ in a 2:1 ratio (Chart 7), whereas the analogous reaction using the PC_5H_4-bridged substrate **3** gave only a mixture of oxidation products. Interestingly, the copper compound **21** did not rearrange into a PC_5H_4-bridged isomer in refluxing 1,2-dichloroethane (as observed for the gold analogue **16**). Definitely, the gold atom plays a critical role at facilitating the complex sequence of P–C and C–H bond cleavage and formation steps needed to accomplish such isomerization.

We have determined crystallographically the structures of the gold complexes **17** and **18** (Figures 6 and 7, Tables 7 and 8)

Chart 7

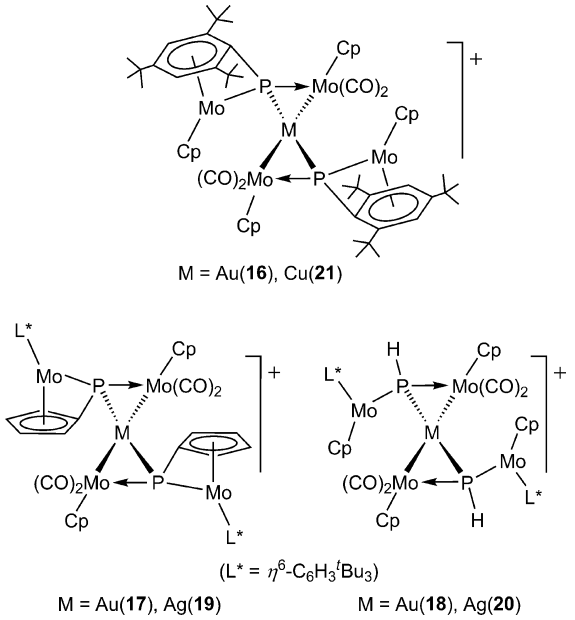

Scheme 2

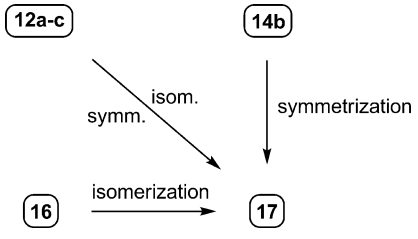

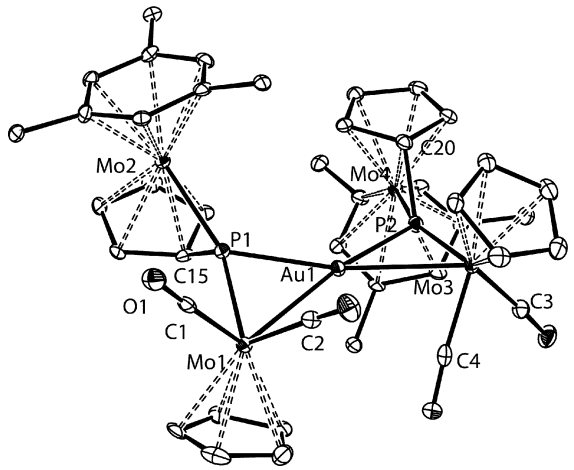

Figure 6. ORTEP diagram (30% probability) of the cation in compound **17** with H atoms and ^{t}Bu groups (except their C^1 atoms) omitted for clarity.

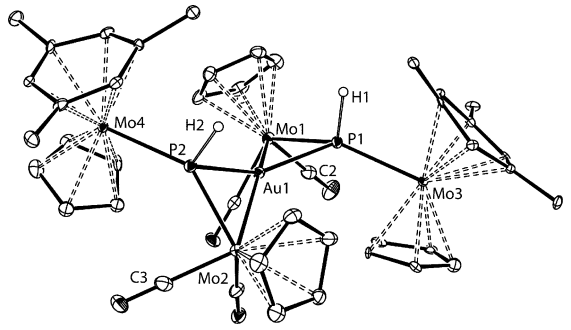

Figure 7. ORTEP diagram (30% probability) of the cation in compound **18** with H atoms (except the P-bound ones) and ^{t}Bu groups (except their C^1 atoms) omitted for clarity.

which in both cases display a distorted bow-tie Mo_2P_2Au central skeleton. We can view these complexes as linear $[D–Au–D]^+$ complexes where the donor D is the π(Mo–P) bonding pair mainly located at the short Mo–P bond of the neutral substrates **3** and **4**. Thus, these pentanuclear complexes can be related to the sandwich complexes $[AuW_2(\mu\text{-}CR)_2L_2(CO)_4]^+$ formed through the coordination of two

dx.doi.org/10.1021/ic501376v | Inorg. Chem. 2014, 53, 10325–10339

Table 7. Selected Bond Lengths (Å) and Angles (deg) for Compound 17

Mo1−Au1	2.8006(7)	Mo1−P1−Mo2	158.0(1)
Mo3−Au1	2.7975(7)	Mo3−P2−Mo4	160.2(1)
Mo1−P1	2.322(2)	P1−Mo1−C1	84.4(3)
Mo1−C1	1.972(9)	P1−Mo1−C2	105.7(3)
Mo1−C2	1.982(10)	P1−Mo1−Au1	56.16(5)
Mo2−P1	2.428(2)	P1−Au1−Mo1	52.00(5)
Mo3−P2	2.322(2)	P1−Au1−Mo3	166.06(5)
Mo3−C3	1.963(9)	P1−Au1−P2	130.62(7)
Mo3−C4	1.967(9)	Mo1−Au1−P2	167.35(5)
Mo4−P2	2.421(2)	Mo1−Au1−Mo3	129.34(2)
Au1−P1	2.448(2)	C1−Mo1−C2	77.5(4)
Au1−P2	2.455(2)	C3−Mo3−C4	76.5(3)
P1−C15	1.789(9)		
P2−C20	1.819(9)		

Table 8. Selected Bond Lengths (Å) and Angles (deg) for Compound 18

Mo1−Au1	2.8233(8)	Mo1−P1−Mo3	146.75(10)
Mo2−Au1	2.8691(7)	Mo2−P2−Mo4	143.59(10)
Mo1−P1	2.360(2)	P1−Mo1−C1	108.9(2)
Mo1−C1	1.965(8)	P1−Mo1−C2	88.5(3)
Mo1−C2	1.941(10)	P1−Mo1−Au1	55.65(5)
Mo3−P1	2.481(2)	P1−Au1−Mo1	52.57(5)
Mo2−P2	2.370(2)	P1−Au1−Mo2	134.53(5)
Mo2−C3	1.941(10)	P1−Au1−P2	151.41(7)
Mo2−C4	1.955(9)	Mo1−Au1−P2	135.58(5)
Mo4−P2	2.485(2)	Mo1−Au1−Mo2	156.92(2)
Au1−P1	2.454(2)	C1−Mo1−C2	80.7(3)
Au1−P2	2.421(2)	C3−Mo2−C4	79.6(4)
P1−H1	1.41(7)		
P2−H2	1.36(7)		

carbyne molecules $[WL(CR)(CO)_2]$ to a single Au^+ ion via the corresponding W≡C bonds (L = Cp or equivalent ligands).[35] Although two different diasteroisomers can be formed in our pentanuclear cations, only one of them is present in the crystal lattice of **17** and **18**, even if displaying a different rotational conformation in either case. In the PC_5H_4-bridged complex **17**, the Mo_2 subunits are arranged roughly head to head with a moderate twist angle of ca. 30° between MoAuP planes. In contrast, the Mo_2 subunits in **18** are rather arranged head to tail around the gold atom and with a larger twist angle of ca. 60° between MoAuP planes. The interatomic Mo−Au, Mo−P, and Au−P distances in **17** and **18** are roughly comparable to the corresponding lengths in the trinuclear complexes **6**, **13b**, and **15d** and therefore deserve no additional comments. We just note that the average Mo−Au lengths in the PH-bridged complex **18** (ca. 2.84 Å) are a bit longer than those in **17** (ca. 2.80 Å), which in turn are slightly longer than the W−Au lengths in the mentioned carbyne complexes (ca. 2.77 Å).[35]

Spectroscopic data in solution for compounds **15** to **21** are broadly consistent with the solid-state structures discussed above, which imply the presence of a binary axis relating corresponding groups of both Mo_2 subunits. In agreement with this, all complexes but the PH-bridged **18** display a single ^{31}P NMR resonance in the range 420−475 ppm, consistent with the presence of μ_3-PR ligands, and a pair of C−O stretching bands in the IR spectrum with the pattern characteristic of cisoid $Mo(CO)_2$ oscillators. The average frequencies of these bands for the gold compounds **15** to **17** are almost identical to those of the neutral AuCl adducts **5** to **8**, while the silver and copper complexes display less energetic bands, as usually observed in heterometallic carbonyl complexes containing group-11 elements. Noticeably, the silver complexes **19** and **20** display ^{31}P chemical shifts some 30 ppm higher than their gold counterparts **17** and **18**, which is the reverse of the usual ordering in compounds containing MPR_3 units, without an obvious reason. The corresponding resonances display at room temperature measurable couplings of ca. 90 and 100 Hz respectively to the Ag nuclei. This indicates the absence of significant dissociation of the neutral Mo_2 subunits of these complexes on the NMR time scale, while the magnitudes of these couplings are lower than the values above 300 Hz usually measured for $AgPR_3$ units bridging dimetal edges in heterometallic clusters.[4b] This can be accounted for by considering the increased coordination number around the silver atom (4) and the tricentric nature of the bond connecting the P and Ag atoms in these compounds.

The ^1H NMR spectrum of the copper complex **21** unexpectedly reveals that both Mo_2 subunits of the molecule are not exactly equivalent, since it displays four Cp resonances and two different sets of resonances for the aryl groups (see the Experimental Section). This might be explained by assuming different local conformations in the Mo_2 subunits (e.g., *syn* and *anti*, as observed for the trinuclear complexes **7**, Chart 4) with accidental degeneracy of the corresponding ^{31}P NMR resonances. Unfortunately, all attempts to grow single crystals for a diffraction study of this complex were unsuccessful.

The PH-bridged gold complex **18** stands apart from the rest of the complexes in that it displays four different isomers in solution in a ratio of ca. 1:6:4:1, as shown by the ^{31}P and ^1H NMR spectra, a circumstance perhaps derived from the smaller steric requirements of the corresponding Mo_2 subunits. This is also reflected in the IR spectrum of this compound, which displays three C−O stretches rather than two. These isomers likely interconvert in solution, since the IR and NMR spectra of the crystals used in the diffraction study displayed the same isomeric mixture, although we have not studied this process in detail. As noted above, two different diastereoisomers are possible when building up these pentanuclear complexes from identical Mo_2 subunits which, when combined with possible *syn* and *anti* local conformations within each Mo_2 subunit yields a total of 12 possible isomers. The four observed isomers of **18** display similar ^{31}P chemical shifts (434−417 ppm) with moderate P−H couplings (224−268 Hz), not far from the values measured for the trinuclear complexes **15**, and also give rise to strongly deshielded proton PH resonances (ca. 10 ppm), all of this being consistent with the presence of μ_3-PH ligands bridging open trimetal units. Each of them seem to give rise to only a pair of Cp resonances (see the Experimental Section), thus implying that the Mo_2 subunits within each isomer must be identical to each other, as found for the isomer present in the crystal lattice.

CONCLUSION

The π(Mo−P) bonding electron pair in the phosphinidene complexes **1** to **4**, which is more located at their short Mo−P bond, makes them good donors to Au(I) centers, thus enabling the formation of heterometallic derivatives with Mo_2Au or Mo_4Au metal cores held by tricentric MoPAu bonds via reactions of compounds **1** to **4** with suitable gold complexes such as the neutral [AuCl(THT)] or the cations $[Au(PR_3)(THT)]^+$ and $[Au(THT)_2]^+$. Related Ag(I) or Cu(I)

dx.doi.org/10.1021/ic501376v | Inorg. Chem. 2014, 53, 10325−10339

complexes could be obtained only in a few cases, due to the operation of undesired redox processes in the corresponding reactions. In contrast to this behavior, reactions with HgI_2 resulted either in coordination of the phosphinidene complex via a nonbonding Mo-based electron pair rendering a dative Mo→Hg interaction (for the more crowded compound **1**) or in oxidative addition of a Hg−I bond to the Mo−P bond of the parent complex (compound **3**). Coordination of gold atoms to the arylphosphinidene complex **1** promotes a complex sequence of P−C and C−H bond formation and cleavage steps in the aryl and cyclopentadienyl groups resulting in the formation of isomeric species having bridging cyclopentadienylidene−phosphinidene (PC_5H_4) ligands.

EXPERIMENTAL SECTION

General Procedures and Starting Materials. All manipulations and reactions were carried out under a nitrogen (99.995%) atmosphere using standard Schlenk techniques. Solvents were purified according to literature procedures and distilled prior to use.[36] The parent compounds $[Mo_2Cp_2(\mu\text{-}\kappa^1\text{:}\kappa^1,\eta^6\text{-PR*})(CO)_2]$ (**1**), $[Mo_2Cp_2(\mu\text{-}\kappa^1\text{:}\kappa^1,\eta^4\text{-PR*})(CO)_3]$ (**2**), $[Mo_2Cp(\mu\text{-}\kappa^1\text{:}\kappa^1,\eta^5\text{-}PC_5H_4)(CO)_2(\eta^6\text{-HR*})]$ (**3**),[11] and $[Mo_2Cp_2(\mu\text{-PH})(CO)_2(\eta^6\text{-HR*})]$ (**4**)[12] were prepared as described before (Cp = η^5-C_5H_5, R* = 2,4,6-$C_6H_2{}^tBu_3$). Complexes $[AuCl(THT)]$,[37] $[AuCl(PR_3)]$,[38] $[AgCl(PPh_3)]_4$,[39] K$[MoCp(CO)_3]$,[40] and $Na(BAr_4')$[41] were also prepared by literature methods (THT = SC_4H_8; Ar′ = 3,5-$C_6H_3(CF_3)_2$), and all other reagents were obtained from the usual commercial suppliers and used as received, unless otherwise stated. Petroleum ether refers to that fraction distilling in the range 338−343 K. Filtrations were carried out through diatomaceous earth unless otherwise indicated. Chromatographic separations were carried out using jacketed columns refrigerated by tap water (ca. 288 K) or by a closed 2-propanol circuit kept at the desired temperature with a cryostat. Commercial aluminum oxide (activity I, 150 mesh) was degassed under a vacuum prior to use. The latter was mixed afterward under nitrogen with the appropriate amount of water to reach the activity desired (activity IV, unless otherwise stated). IR stretching frequencies of CO ligands were measured in solution, using CaF_2 windows. Nuclear Magnetic Resonance (NMR) spectra were routinely recorded at 300.13 (^{1}H), 121.50 (^{31}P{^{1}H}), or 75.47 MHz (^{13}C{^{1}H}) at 295 K in CD_2Cl_2 solution unless otherwise stated. Chemical shifts (δ) are given in parts per million, relative to internal tetramethylsilane (^{1}H, ^{13}C) or external 85% aqueous H_3PO_4 (^{31}P). Coupling constants (J) are given in Hertz.

Preparation of $[AuMo_2ClCp_2(\mu\text{-}\kappa^1\text{:}\kappa^1\text{:}\kappa^1,\eta^6\text{-PR*})(CO)_2]$ (5) and $[AuMo_2ClCp(\mu\text{-}\kappa^1\text{:}\kappa^1\text{:}\kappa^1,\eta^5\text{-}PC_5H_4)(CO)_2(\eta^6\text{-HR*})]$ (7). Solid $[AuCl(THT)]$ (0.010 g, 0.031 mmol) was added to a dichloromethane solution (3 mL) of compound **1** (0.020 g, 0.030 mmol), and the mixture was stirred for 1 min to give a bright red solution. Solvent was then removed under a vacuum, and the residue was extracted with CH_2Cl_2/petroleum ether (1/1, 10 mL) and the extract filtered. Removal of solvents from the filtrate under a vacuum gave a solid shown (by ^{31}P and ^{1}H RMN) to be a mixture of the isomers **5** and **7** in a **5**/**7** ratio of ca. 5. Full isomerization of **5** into **7** was accomplished by heating the above mixture in 1,2-dichloroethane solution (3 mL) at 313 K for 10 min. The violet resulting solution was then filtered and solvent removed under vacuum from the filtrate to give compound **7** (0.022 g, 82%) as a violet solid. Compound **7** displays in solution two interconverting isomers (*syn* and *anti*) with the *syn*/*anti* ratio being ca. 1/5 in toluene-d_8 at 273 K. *Data for* **5**: ^{1}H NMR: δ 5.77, 5.72 (2s, br, 2 × 1H, C_6H_2), 5.50 (s, 5H, Cp), 5.19 (d, J_{PH} = 2, 5H, Cp), 1.32, 1.26, 1.22 (3s, 3 × 9H, ^{t}Bu). *Data for* **7**: Anal. Calcd for $C_{30}H_{39}AuClMo_2O_2P$: C, 40.63; H, 4.43. Found: C, 40.22; H, 4.60. ^{31}P{^{1}H} NMR (C_6D_6): δ 377.3 (s, br, *syn*), 370.1 (s, br, *anti*). ^{1}H NMR (CD_2Cl_2, 400.13 MHz, *anti* isomer): δ 5.58 (s, 5H, Cp), 5.39 (m, 2H, C_5H_4), 5.20 (s, br, 3H, C_6H_3), 4.93, 4.37 (2m, 2 × 1H, C_5H_4), 1.26 (s, 27H, ^{t}Bu). ^{1}H NMR (toluene-d_8, 273 K, *anti* isomer): δ 5.04 (s, br, 3H, C_6H_3), 4.96 (s, 5H, Cp), 4.74 (m, 2H, C_5H_4), 4.64, 3.93 (2m, 2 × 1H, C_5H_4), 1.12 (s, 27H, ^{t}Bu). ^{13}C{^{1}H} NMR (100.63 MHz, toluene-d_8, 273 K, *anti* isomer): δ 240.0 (s, 2MoCO), 112.9 [s, C(C_6H_3)], 91.4 (s, Cp), 88.6, 87.6, 82.2, 78.9 [4s, CH(C_5H_4)], 76.4 [s, CH(C_6H_3)], 34.8 [s, C^1(^{t}Bu)], 31.5 [s, C^2(^{t}Bu)]; the resonance for the C^1 atom of the PC_5H_4 ligand could not be identified in this spectrum. ^{1}H NMR (toluene-d_8, 273 K, *syn* isomer): δ 5.14 (s, 5H, Cp), 1.02 (s, 27H, ^{t}Bu). ^{13}C{^{1}H} NMR (100.63 MHz, toluene-d_8, 273 K, *syn* isomer): δ 237.4 (s, 2MoCO), 110.6 [s, C(C_6H_3)], 92.6 (s, Cp), 77.5 [s, CH(C_6H_3)]; other resonances for this minor isomer were obscured by those of the major isomer.

Preparation of $[AuMo_2ClCp_2(\mu\text{-}\kappa^1\text{:}\kappa^1\text{:}\kappa^1,\eta^4\text{-PR*})(CO)_3]$ (6). Solid $[AuCl(THT)]$ (0.008 g, 0.025 mmol) was added to a dichloromethane solution (3 mL) of compound **2** (0.015 g, 0.022 mmol), and the mixture was stirred for 1 min to give a bright red solution which was filtered with a canula. Removal of solvent from the filtrate under a vacuum gave compound **6** as a red solid (0.014 g, 70%). The crystals of **6** used in the X-ray diffraction study were grown by the slow diffusion of layers of toluene and petroleum ether into a concentrated dichloromethane solution of the complex at 253 K. Anal. Calcd for $C_{31}H_{39}AuClMo_2O_3P$: C, 40.70; H, 4.30. Found: C, 40.53; H, 4.25. ^{1}H NMR: δ 6.09 (s, 1H, C_6H_2), 5.98 (d, J_{HP} = 2, 1H, C_6H_2), 5.58, 5.39 (2s, 2 × 5H, Cp), 1.39, 1.22, 1.04 (3s, 3 × 9H, ^{t}Bu).

Preparation of $[AuMo_2ClCp(\mu_3\text{-PH})(CO)_2(\eta^6\text{-HR*})]$ (8). Solid $[AuCl(THT)]$ (0.013 g, 0.040 mmol) was added to a dichloromethane solution (4 mL) of compound **4** (0.026 g, 0.040 mmol) at 213 K, and the mixture was stirred for 5 min to give a violet solution which was filtered with a canula. Removal of the solvent from the filtrate under a vacuum and washing of the residue with petroleum ether (2 × 5 mL) gave compound **8** as a violet solid (0.031 g, 88%). Anal. Calcd for $C_{30}H_{41}AuClMo_2O_2P$: C, 40.54; H, 4.65. Found: C, 40.70; H, 4.75. ^{31}P NMR: δ 357.7 (d, J_{HP} = 238, μ_3-PH). ^{1}H NMR: δ 9.06 (d, J_{HP} = 238, 1H, μ_3-PH), 5.50 (s, br, 5H, Cp), 5.00 (d, J_{HP} = 6, 3H, C_6H_3), 4.98 (d, J_{HP} = 4, 5H, Cp), 1.27 (s, 27H, ^{t}Bu).

Preparation of $[AuMo_3Cp_2(\mu\text{-}\kappa^1\text{:}\kappa^1\text{:}\kappa^1,\eta^5\text{-}PC_5H_4)(CO)_5(\eta^6\text{-HR*})]$ (9). A solution of K$[MoCp(CO)_3]$ (0.015 g, 0.053 mmol) in tetrahydrofuran (2 mL) was added to a tetrahydrofuran solution (5 mL) of compound **7** (0.034 g, 0.038 mmol) previously cooled at 213 K, and the mixture was stirred at this temperature for 10 min to give a green solution. After removal of the solvent under a vacuum, the residue was extracted with dichloromethane/petroleum ether (1/4), and the extracts were chromatographed on alumina at 288 K. Elution with dichloromethane/petroleum ether (1/10) gave a green fraction yielding, after removal of solvents, compound **9** as a green microcrystalline solid (0.037 g, 89%). This complex displays in solution two interconverting isomers (*syn* and *anti*), with the *syn*/*anti* ratio being ca. 1/5 in toluene-d_8 at 233 K. Anal. Calcd for $C_{38}H_{44}AuMo_3O_5P$: C, 41.62; H, 4.04. Found: C, 41.25; H, 3.87. ^{31}P{^{1}H} NMR (162.06 MHz, toluene-d_6, 293 K): δ 391.4 (s, br, *syn*), 373.5 (s, br, *anti*). ^{1}H NMR (400.13 MHz, averaged spectrum): δ 5.63 (s, 5H, Cp), 5.39 (m, 1H, C_5H_4), 5.28 (s, 5H, Cp), 5.20 (s, br, 3H, C_6H_3), 5.08 (m, br, 2H, C_5H_4), 4.27 (m, vbr, 1H, C_5H_4), 1.27 (s, 27H, ^{t}Bu). ^{13}C{^{1}H} NMR (100.63 MHz, averaged spectrum): δ 244.8 (s, MoCO), 244.4 (s, MoCO), 231.4 (s, 3MoCO), 113.8 [s, C(C_6H_3)], 93.3 [s, C^1(C_5H_4)], 88.9 (s, 2Cp), 89.6, 88.3, 83.2, 78.9 [4s, CH(C_5H_4)], 73.7 [s, CH(C_6H_3)], 35.2 [s, C^1(^{t}Bu)], 31.6 [s, C^2(^{t}Bu)]. *Data for isomer anti*: ^{1}H NMR (400.13 MHz, toluene-d_6, 233 K): δ 5.34 (m, 1H, C_5H_4), 5.32, 5.18 (2s, 2 × 5H, Cp), 5.00 (s, br, 3H, C_6H_3), 4.70, 4.44, 3.82 (3m, 3 × 1H, C_5H_4), 1.09 (s, 27H, ^{t}Bu). *Data for isomer syn*: ^{1}H NMR (400.13 MHz, toluene-d_6, 233 K): δ 5.50 (m, 1H, C_5H_4), 5.44, 5.08 (2s, 2 × 5H, Cp), 4.67 (s, br, 3H, C_6H_3), 4.78, 4.70, 4.55 (3m, 3 × 1H, C_5H_4), 0.99 (s, 27H, ^{t}Bu).

Preparation of $[HgMo_2Cp_2(\mu\text{-I})I(\mu\text{-}\kappa^1\text{:}\kappa^1,\eta^6\text{-PR*})(CO)_2]_2$ (10). Solid HgI_2 (0.018 g, 0.040 mmol) was added to a solution of compound **1** (0.025 g, 0.038 mmol) in dichloromethane (3 mL), and the mixture was stirred for 1 min to give a brick-red solution which was chromatographed on alumina at 285 K. Elution with dichloromethane gave a red fraction yielding, after removal of the solvent under a vacuum, compound **10** as a brick-red microcrystalline solid (0.038g, 90%). The crystals of **10** used in the X-ray diffraction study were grown by the slow diffusion of a layer of toluene into a concentrated dichloromethane solution of the complex at 253 K. Anal. Calcd for

dx.doi.org/10.1021/ic501376v | Inorg. Chem. 2014, 53, 10325−10339

$C_{30}H_{39}HgI_2Mo_2O_2P$: C, 32.49; H, 3.55. Found: C, 32.35; H, 3.40. ^{1}H NMR (400.13 MHz): δ 5.92 (s, 2H, C_6H_2), 5.59, 5.52 (2s, 2 × 5H, Cp), 1.30 (s, 18H, ^{t}Bu), 1.27 (s, 9H, ^{t}Bu).

Preparation of [HgMo$_2$CpI$_2$(μ-κ^1:κ^1:κ^1,η^5-PC$_5$H$_4$)(CO)$_2$(η^6-HR*)] (11). Solid HgI_2 (0.018 g, 0.040 mmol) was added to a solution of compound **3** (0.025 g, 0.038 mmol) in dichloromethane (3 mL), and the mixture was stirred for 1 min to give a yellow-brown solution shown by NMR to contain compound **11** as a major product. This complex, however, turned out to be quite susceptible to hydrolysis, and all attempts to further purify it resulted in its progressive decomposition. IR and ^{31}P NMR data for this compound are given in Table 2.

Preparation of [AuMo$_2$Cp$_2$(μ-κ^1:κ^1:κ^1,η^6-PR*)(CO)$_2$(THT)](PF$_6$) (12a). A dichloromethane solution (5 mL) of [Au(THT)$_2$](PF$_6$) (0.040 mmol) was prepared in situ by stirring [AuCl(THT)] (0.013 g, 0.040 mmol) and TlPF$_6$ (0.014g, 0.040 mmol) in the presence of THT (0.1 mL, excess) for 5 min. The solution was filtered using a canula and then added to a solution of compound **1** (0.025 g, 0.038 mmol) in dichloromethane (1 mL), to give a red solution instantaneously. Solvent was then removed under a vacuum, the residue was extracted with dichloromethane (15 mL), and the extract was filtered with a canula. Removal of the solvent from the filtrate gave compound **12a** as a red microcrystalline solid (0.032 g, 77%). Anal. Calcd for $C_{34}H_{47}AuF_6Mo_2O_2P_2S$: C, 37.65; H, 4.37. Found: C, 37.62; H, 4.40. ^{1}H NMR: δ 5.88 (s, br, 2H, C_6H_2), 5.55, 5.24 (2s, 2 × 5H, Cp), 3.43, 2.16 (2m, br, 2 × 4H, CH_2), 1.46, 1.36 (2s, br, 2 × 9H, *o*-^{t}Bu), 1.26 (s, 9H, *p*-^{t}Bu).

Preparation of [AuMo$_2$Cp$_2$(μ-κ^1:κ^1:κ^1,η^6-PR*)(CO)$_2${P(*p*-tol)$_3$}](PF$_6$) (12b). A tetrahydrofuran solution (4 mL) of [Au{P(*p*-tol)$_3$}(THT)](PF$_6$) (0.040 mmol) was prepared in situ by stirring [AuCl{P(*p*-tol)$_3$}] (0.022 g, 0.040 mmol) and TlPF$_6$ (0.014 g, 0.040 mmol) in the presence of THT (0.05 mL, excess) for 10 min. The solution was filtered using a canula and then added to solid compound **1** (0.025 g, 0.038 mmol), and the mixture was stirred for 1 min to give a red solution. Solvent was then removed under a vacuum; the residue was washed with a 1:1 diethyl ether/petroleum ether mixture (3 × 5 mL), then extracted with a 1:1 toluene/dichloromethane mixture (3 × 5 mL) and the extracts filtered with a canula. Removal of solvents from the filtrate gave compound **12b** as a red microcrystalline solid (0.030 g, 60%). Anal. Calcd for $C_{51}H_{60}AuF_6Mo_2O_2P_3$: C, 47.09; H, 4.65. Found: C, 46.87; H, 4.70. ^{1}H NMR: δ 7.40−7.30 (m, 12H, C_6H_4), 5.86 (s, 2H, C_6H_2), 5.53 (s, 5H, Cp), 5.16 (s, br, 5H, Cp), 2.43 (s, 9H, C_6H_4*Me*), 1.26 (s, br, 27H, ^{t}Bu). ^{13}C{^{1}H} NMR: δ 143.3 [s, C^4(*p*-tol)], 134.0 [d, J_{CP} = 14, CH(*p*-tol)], 130.5 [d, J_{CP} = 12, CH(*p*-tol)], 126.6 [d, J_{CP} = 54, C^1(*p*-tol)], 109.0 [s, C(C_6H_2)], 105.9 [s, C(C_6H_2)], 92.9 (s, br, Cp), 89.9 (s, Cp), 85.5 [d, J_{CP} = 60, C^1(C_6H_2)], 83.7 [s, br, 2CH(C_6H_2)], 35.4 [s, 2C^1(^{t}Bu)], 31.9 [s, C^2(^{t}Bu)], 31.4 [s, C^1(^{t}Bu)], 23.1 [s, 2C^2(^{t}Bu)], 21.6 [s, C_6H_4*Me*]; the carbonyl resonances could not be identified clearly in this spectrum.

Preparation of [AuMo$_2$Cp$_2$(μ-κ^1:κ^1:κ^1,η^6-PR*)(CO)$_2$(PMe$_3$)](PF$_6$) (12c). The procedure is analogous to that described for **12b**, but using [AuCl(PMe$_3$)] (0.012 g, 0.039 mmol) instead. Solvent was removed under a vacuum from the resulting red solution. The residue was extracted with a 1:1 toluene/dichloromethane mixture (3 × 5 mL), and the extracts were filtered with a canula. Removal of the solvents from the filtrate gave compound **12c** as a red microcrystalline solid (0.030 g, 73%). Anal. Calcd for $C_{33}H_{48}AuF_6Mo_2O_2P_3$: C, 36.96; H, 4.51. Found: C, 37.20; H, 4.72. ^{1}H NMR: δ 5.89 (s, 2H, C_6H_2), 5.53, 5.26 (2s, 2 × 5H, Cp), 1.67 (d, J_{HP} = 11, 9H, Me), 1.39 (s, 18H, ^{t}Bu), 1.27 (s, 9H, ^{t}Bu).

Preparation of [AuMo$_2$Cp$_2$(μ-κ^1:κ^1:κ^1,η^4-PR*)(CO)$_3$(THT)](PF$_6$) (13a). The procedure is analogous to that described for **12a**, but using compound **2** (0.025 g, 0.037 mmol) instead. After similar workup, compound **13a** was obtained as a red microcrystalline solid (0.035 g, 85%). Anal. Calcd for $C_{35}H_{47}AuF_6Mo_2O_3P_2S$: C, 37.78; H, 4.26. Found: C, 37.46; H, 4.48. ^{1}H NMR: δ 6.11, 6.10 (2s, 2 × 1H, C_6H_2), 5.65 (s, 5H, Cp), 5.48 (d, J_{HP} = 3, 5H, Cp), 3.40, 2.12 (2m, 2 × 4H, THT), 1.39, 1.21, 1.05 (3s, 3 × 9H, ^{t}Bu). ^{13}C{^{1}H} NMR (100.63 MHz): δ 240.3 [d, J_{PC} = 27, MoCO], 238.2 (s, MoCO), 233.5 [d, J_{CP} = 5, MoCO], 156.7 [s, C^6(C_6H_2)], 131.9 [s, C^5(C_6H_2)], 112.5 [s, br C^4(C_6H_2)], 110.1 [s, C^2(C_6H_2)], 93.5 (s, br, Cp), 93.0 (s, Cp), 86.5 [s, C^3(C_6H_2)], 76.0 [d, J_{CP} = 44, C^1(C_6H_2)], 41.0 [s, C^1(^{t}Bu)], 39.1 (s, br, SCH_2), 36.1, 35.9 [2s, C^1(^{t}Bu)], 34.0, 32.2 [2s, C^2(^{t}Bu)], 31.3 (s, br, CH_2), 31.2 [s, C^2(^{t}Bu)].

Preparation of [AuMo$_2$Cp$_2$(μ-κ^1:κ^1:κ^1,η^4-PR*)(CO)$_3${P(*p*-tol)$_3$}](PF$_6$) (13b). The procedure is analogous to that described for **12b**, but using compound **2** (0.028 g, 0.040 mmol) instead, and dichloromethane as a solvent (5 mL). The red resulting solution was filtered using a canula and the solvent removed from the filtrate under a vacuum. Washing of the residue with petroleum ether yielded compound **13b** as a red microcrystalline solid (0.043 g, 80%). The crystals of **13b** used in the X-ray study were grown by the slow diffusion of layers of diethyl ether and petroleum ether into a concentrated dichloromethane solution of the complex at 253 K. Anal. Calcd for $C_{52}H_{60}AuF_6Mo_2O_3P_3$: C, 47.00; H, 4.55. Found: C, 46.77; H, 4.39. ^{1}H NMR (400.13 MHz): δ 7.46−7.20 (m, 12H, C_6H_4), 6.12, 6.03 (2s, 2 × 1H, C_6H_2), 5.62, 5.42 (2s, 2 × 5H, Cp), 2.45 (s, 9H, C_6H_4*Me*), 1.40, 1.08, 1.02 (3s, 3 × 9H, ^{t}Bu).

Preparation of [AuMo$_2$Cp(μ-κ^1:κ^1:κ^1,η^5-PC$_5$H$_4$)(CO)$_2$(η^6-HR*)-{P(*p*-tol)$_3$}](PF$_6$) (14b). The procedure is analogous to that described for **12b**, but using compound **3** (0.023 g, 0.035 mmol) instead. Solvent was removed under a vacuum from the resulting green solution, the residue was extracted with a 1:1 toluene/dichloromethane mixture (3 × 5 mL), and the extracts were filtered with a canula. Removal of solvents from the filtrate gave compound **14b** as a green solid that could not be isolated as a pure substance since it rapidly evolves in solution to give compound **17**. ^{1}H NMR (400.13 MHz): δ 7.40−7.20 (m, 12H, C_6H_4), 5.62 (s, 5H, Cp), 5.31 (s, br, 5H, C_6H_3 and C_5H_4), 4.57, 4.44 (2m, 2 × 1H, C_5H_4), 2.41 (s, 9H, C_6H_4*Me*), 1.19 (s, br, 27H, ^{t}Bu).

Preparation of [AuMo$_2$Cp$_2$(μ_3-PH)(CO)$_2$(η^6-HR*){P(*p*-tol)$_3$}](BAr′$_4$) (15b). A dichloromethane solution (5 mL) of [Au{P(*p*-tol)$_3$}(THT)](BAr′$_4$) (0.040 mmol) was prepared in situ by stirring [AuCl{P(*p*-tol)$_3$}] (0.022 g, 0.040 mmol) and Na(BAr′$_4$) (0.035g, 0.040 mmol) in the presence of THT (0.05 mL, excess) for 10 min. The solution was filtered using a canula and then added to a solution of compound **4** (0.026 g, 0.040 mmol) in dichloromethane (5 mL) at 213 K, to give a blue solution instantaneously. Solvent was then removed under a vacuum; the residue was extracted with dichloromethane/petroleum ether (5:1) and the extracts chromatographed on alumina at 253 K. Elution with the same mixture gave a blue fraction yielding, after removal of solvents, compound **15b** as a blue microcrystalline solid (0.075 g, 93%). Anal. Calcd for $C_{83}H_{74}AuBF_{24}Mo_2O_2P_2$: C, 49.33; H, 3.69. Found: C, 49.19; H, 3.60. ^{1}H NMR: δ 10.47 (d, J_{HP} = 233, 1H, μ_3-PH), 7.73 (m, 8H, Ar′), 7.56 (s, br, 4H, Ar′), 7.40−7.18 (m, 12H, C_6H_4), 5.55 (s, 5H, Cp), 5.08 (d, J_{HP} = 5, 3H, C_6H_3), 5.01 (d, J_{HP} = 3, 5H, Cp), 2.41 (s, 9H, C_6H_4*Me*), 1.17 (s, 27H, ^{t}Bu). ^{31}P NMR: δ 425.0 (dd, J_{HP} = 233, J_{PP} = 65, μ_3-PH), 60.4 [d, J_{PP} = 65, AuP].

Preparation of [AuMo$_2$Cp$_2$(μ_3-PH)(CO)$_2$(η^6-HR*)(PMe$_3$)](BAr′$_4$) (15c). The procedure is analogous to that one described for **15b**, but using [AuCl(PMe$_3$)}] (0.013 g, 0.040 mmol) instead. After a similar workup, compound **15c** was obtained as a blue microcrystalline solid (0.067 g, 93%). Anal. Calcd for $C_{65}H_{62}AuBF_{24}Mo_2O_2P_2$: C, 43.55; H, 3.49. Found: C, 43.41; H, 3.39. ^{1}H NMR: δ 10.15 (dd, J_{HP} = 234, J_{HP} = 3, 1H, μ_3-PH), 7.72 (m, 8H, Ar′), 7.56 (s, br, 4H, Ar′), 5.57 (s, 5H, Cp), 5.12 (d, J_{HP} = 5, 3H, C_6H_3), 5.05 (d, J_{HP} = 5, 5H, Cp), 1.50 (d, J_{HP} = 10, 9H, PMe), 1.25 (s, 27H, ^{t}Bu). ^{31}P NMR: δ 416.6 (dd, J_{HP} = 234, J_{PP} = 68, μ_3-PH), 30.7 (d, J_{PP} = 68, AuP). ^{13}C{^{1}H} NMR: δ 242.4 (d, J_{CP} = 27, MoCO), 239.1 (s, MoCO), 161.9 [q, J_{CB} = 50, C^1(Ar′)], 135.0 [s, C^2(Ar′)], 129.0 [q, J_{CF} = 32, C^3(Ar′)], 124.7 (q, J_{CF} = 272, CF_3), 117.6 [s, C^4(Ar′)], 112.3 [s, C(C_6H_3)], 93.1, 86.3 (2s, Cp), 83.0 [s, CH(C_6H_3)], 35.3 [s, C^1(^{t}Bu)], 31.9 [s, C^2(^{t}Bu)], 15.5 (d, J_{CP} = 32, PMe).

Preparation of [AuMo$_2$Cp$_2$(μ_3-PH)(CO)$_2$(η^6-HR*)(P^{i}Pr$_3$)](BAr′$_4$) (15d). The procedure is analogous to that one described for **15b**, but using [AuCl(P^{i}Pr$_3$)}] (0.016 g, 0.040 mmol) instead. After a similar workup, compound **15d** was obtained as a blue microcrystalline solid (0.068 g, 90%). The crystals of **15d** used in the X-ray diffraction study were grown by the slow diffusion of layers of diethyl ether and

dx.doi.org/10.1021/ic501376v | Inorg. Chem. 2014, 53, 10325−10339

Table 9. Crystal Data for New Compounds

	6·2CH_2Cl_2	**9**·1/3C_7H_8	**10**·2CH_2Cl_2	**13b**	**15d**·1/2C_6H_{14}	**17**·2CH_2Cl_2	**18**·3Et_2O
mol formula	$C_{32}H_{41}AuCl_3Mo_2O_3P$	$C_{121}H_{140}Au_3Mo_9O_{15}P_3$	$C_{62}H_{82}Cl_4Hg_2I_4Mo_4O_4P_2$	$C_{52}H_{60}AuF_6Mo_2O_3P_3$	$C_{74}H_{81}AuBF_{24}Mo_2O_2P_2$	$C_{62}H_{82}AuCl_4F_6Mo_4O_4P_3$	$C_{104}H_{121}AuBF_{24}Mo_4O_7P_2$
mol wt	999.82	3381.62	2387.56	1328.76	1919.98	1820.71	2592.49
cryst syst	monoclinic	triclinic	triclinic	triclinic	triclinic	monoclinic	monoclinic
space group	$P2_1/c$	$P\bar{1}$	$P\bar{1}$	$P\bar{1}$	$P\bar{1}$	$P2_1/c$	$P2_1/c$
radiation (λ, Å)	0.71073	0.71073	0.71073	1.54184	1.54184	0.71073	0.71073
a, Å	15.3672(4)	18.113(2)	10.8045(7)	14.5626(4)	13.8275(5)	17.5559(2)	10.2449(3)
b, Å	11.6754(2)	18.381(2)	13.6911(8)	14.6607(4)	16.9809(6)	11.5363(2)	49.4211(16
c, Å	20.7559(6)	18.613(2)	26.0039(17)	15.5464(4)	17.6409(8)	36.3141(6)	21.4992(8)
α, deg	90	92.177(6)	90.079(3)	65.608(2)	75.786(3)	90	90
β, deg	109.0060(10)	92.230(6)	95.095(2)	86.950(2)	83.330(3)	101.0760(10)	100.297(2)
γ, deg	90	90.789(6)	106.489(3)	62.080(3)	74.395(3)	90	90
V, Å^3	3520.97(15)	6187.0(12)	3672.4(4)	2630.18(16)	3861.8(3)	7217.71(19)	10710.0(6)
Z	4	2	2	2	2	4	4
calcd density, g cm^{-3}	1.886	1.815	2.159	1.678	1.651	1.676	1.61
absorp coeff, mm^{-1}	5.162	4.516	6.739	10.368	7.415	2.973	1.944
temp, K	100	100	100	100	100	100	100
θ range (deg)	1.4–26.48	1.1–26.42	1.55–25.24	3.17–74.09	2.59–73.82	1.14–25.24	0.82–26.4
index ranges (h, k, l)	−18, 17; −14, 0; −25, 16	−22, 22; −22, 22; 0, 23	−12, 12; −16, 16; 0, 31	−18, 18; −18, 18; −19, 17	−17, 16; −20, 21; −21, 20	−21, 20; 0, 13; 0, 43	−12, 12; 0, 61; 0, 26
no. of reflns collected	28269	99855	35340	41414	32372	60631	95432
no. of indep reflns (R_{int})	6340 (0.0481)	21408 (0.0800)	11633 (0.0304)	10645 (0.0389)	14100(0.0735)	12961(0.0525)	21934(0.1190)
reflns with $I > 2\sigma(I)$	5632	14670	7332	9469	8047	10023	13461
R indexes [data with $I > 2\sigma(I)$][a]	R_1 = 0.0358; wR_2 = 0.1132[b]	R_1 = 0.072; wR_2 = 0.1785[c]	R_1 = 0.0653; wR_2 = 0.166[d]	R_1 = 0.0328; wR_2 = 0.085[e]	R_1 = 0.047; wR_2 = 0.0977[f]	R_1 = 0.0548; wR_2 = 0.1594[g]	R_1 = 0.0632; wR_2 = 0.1132[h]
R indexes (all data)[a]	R_1 = 0.0408; wR_2 = 0.1156[b]	R_1 = 0.1162; wR_2 = 0.1954[c]	R_1 = 0.0941; wR_2 = 0.213[d]	R_1 = 0.0376; wR_2 = 0.0891[c]	R_1 = 0.0936; wR_2 = 0.1138[f]	R_1 = 0.0685; wR_2 = 0.1713[g]	R_1 = 0.1244; wR_2 = 0.141[h]
GOF	1.19	0.913	1.065	1.044	0.863	1.154	1.029
no. of restraints/params	0/386	333/1373	0/742	0/624	0/964	0/328	60/1319
$\Delta\rho$ (max., min.), eÅ^{-3}	1.823, −2.754	6.598, −3.419	6.643, −3.408	1.143, −1.733	1.401, −2.061	1.907, −2.675	2.621, −1.104

[a] $R = \Sigma||F_o| - |F_c||/\Sigma|F_o|$. $wR = [\Sigma w(|F_o|^2 - |F_c|^2)^2/\Sigma w|F_o|^2]^{1/2}$. $w = 1/[\sigma^2(F_o^2) + (aP)^2 + bP]$ where $P = (F_o^2 + 2F_c^2)/3$. [b] $a = 0.0668$, $b = 7.2126$. [c] $a = 0.0730$, $b = 390.0522$. [d] $a = 0.1400$, $b = 0.0000$. [e] $a = 0.0567$, $b = 3.5138$. [f] $a = 0.0506$, $b = 0.0000$. [g] $a = 0.0968$, $b = 27.5560$. [h] $a = 0.0421$, $b = 48.2068$.

dx.doi.org/10.1021/ic501376v | Inorg. Chem. 2014, 53, 10325−10339

petroleum ether into a concentrated dichloromethane solution of the complex at 253 K. Anal. Calcd for $C_{71}H_{74}AuBF_{24}Mo_2O_2P_2$: C, 45.43; H, 3.97. Found: C, 45.18; H, 3.81. ^{1}H NMR: δ 10.34 (d, J_{HP} = 232, 1H, μ_3-PH), 7.72 (m, 8H, Ar′), 7.56 (s, br, 4H, Ar′), 5.54 (s, 5H, Cp), 5.08 (d, br, J_{HP} = 4, 8H, Cp and C_6H_3), 2.41 (m, 3H, ^{i}Pr), 1.29−1.25 (m, 18H, ^{i}Pr), 1.24 (s, 27H, ^{t}Bu). ^{31}P NMR: δ 422.7 (dd, J_{HP} = 232, J_{PP} = 60, μ_3-PH), 92.2 (d, J_{PP} = 60, AuP).

Preparation of [Au{$Mo_2Cp_2(\mu$-κ^1:κ^1:κ^1,η^6-PR*)$(CO)_2$}$_2$][PF_6] (16). A dichloromethane solution (5 mL) of [$Au(THT)_2$][PF_6] (0.016 mmol) was prepared in situ as described for **12a**. The solution was filtered using a canula and then added to a solution of compound **1** (0.020 g, 0.031 mmol) in dichloromethane (1 mL), to give a red solution instantaneously, which was further stirred for 5 min. Solvent was then removed under a vacuum. The residue was washed with petroleum ether (3 × 5 mL), then extracted with dichloromethane (10 mL), and the extract was filtered with a canula. Removal of the solvent from the filtrate gave compound **16** as a red microcrystalline solid (0.022 g, 85%). Anal. Calcd for $C_{60}H_{78}AuF_6Mo_4O_4P_3$: C, 43.65; H, 4.76. Found: C, 43.30; H, 4.50. ^{1}H NMR: δ 5.84 (s, br, 2H, C_6H_2), 5.57 (s, 5H, Cp), 5.38 (s, br, 5H, Cp), 1.36 (s, br, 18H, ^{t}Bu), 1.25 (s, 9H, ^{t}Bu).

Preparation of [Au{$Mo_2Cp(\mu$-κ^1:κ^1:κ^1,η^5-PC_5H_4)$(CO)_2(\eta^6$-HR*)}$_2$][PF_6] (17). The procedure is analogous to that described for **16** but using compound **3** (0.023 g, 0.035 mmol) instead. After a similar workup, compound **17** was obtained as a green microcrystalline solid (0.020 g, 69%). The crystals of **17** used in the X-ray study were grown by the slow diffusion of layers of diethyl ether and petroleum ether into a concentrated dichloromethane solution of the complex at 253 K. Anal. Calcd for $C_{60}H_{78}AuF_6Mo_4O_4P_3$: C, 43.65; H, 4.76. Found: C, 43.42; H, 4.62. ^{1}H NMR: δ 5.68 (s, 5H, Cp), 5.36, 5.17, 5.09, 4.10 (4m, 4 × 1H, C_5H_4), 1.27 (s, br, 27H, ^{t}Bu). ^{1}H NMR (400.13 MHz, 233 K): δ 5.90, 5.74 (2s, 2 × 1H, C_6H_3), 5.69 (s, 5H, Cp), 5.34, 5.18, 5.08 (3m, 3 × 1H, C_5H_4), 4.46 (s, 1H, C_6H_3), 4.11 (m, 1H, C_5H_4), 1.48, 1.23, 1.15 (3s, 3 × 9H, ^{t}Bu).

Preparation of [Au{$Mo_2Cp_2(\mu_3$-PH)$(CO)_2(\eta^6$-HR*)}$_2$][BAr′$_4$] (18). A dichloromethane solution (5 mL) of [$Au(THT)_2$][BAr′$_4$] (0.020 mmol) was prepared in situ by stirring [AuCl(THT)] (0.006 g, 0.020 mmol) and Na(BAr′$_4$) (0.018 g, 0.020 mmol) in the presence of THT (0.05 mL, excess) for 10 min. The solution was filtered using a canula and then added to a solution of compound **4** (0.026 g, 0.040 mmol) in dichloromethane (5 mL) at 213 K, to give a green solution instantaneously. Solvent was then removed under a vacuum; the residue was extracted with dichloromethane/petroleum ether (1/4) and the extracts chromatographed on alumina (activity IV) at 253 K. Elution with the same mixture gave a green fraction yielding, after the removal of solvents, compound **18** as a green microcrystalline solid (0.040 g, 84%). This compound was shown (by NMR) to exist in solution as a mixture of isomers **A** to **D** in a ratio **A**/**B**/**C**/**D** of ca. 1:6:4:1 (CD_2Cl_2, 203 K). The crystals of **18** used in the X-ray study were grown by the slow diffusion of a layer of petroleum ether into a concentrated diethyl ether solution of the mixture of isomers at 253 K. Anal. Calcd for $C_{92}H_{94}AuBF_{24}Mo_4O_4P_2$: C, 46.56; H, 3.99. Found: C, 46.67; H, 4.11. ^{1}H NMR (203 K): δ 10.22 (d, J_{PH} = 268, μ_3-PH, **A**), 10.01 (d, J_{PH} = 226, μ_3-PH, **B**), 9.90 (d, J_{PH} = 224, μ_3-PH, **C**), 7.72 (m, Ar′), 7.56 (s, br, Ar′), 5.75 (s, br, Cp, **A**), 5.47 (s, br, Cp, **B** and **C**), 5.04 (s, br, Cp, **B** and **C**), 4.97 (s, br, C_6H_3, **B** and **C**), 4.92 (s, br, C_6H_3, **A**), 4.69 (s, br, Cp, **A**), 1.27 (s, ^{t}Bu, **A**), 1.24 (s, ^{t}Bu, **B** and **C**). The resonances for the minor isomer **D** could not be identified in this spectrum, they being probably masked by those of the major isomers. ^{31}P{^{1}H} NMR: δ 433.8, 427.6, 423.6, 417.4 (4s, μ_3-PH, isomers **A** to **D** respectively). ^{31}P NMR: δ 433.8 (d, J_{HP} = 268, **A**), 427.6 (d, J_{HP} = 226, **B**), 423.6 (d, J_{HP} = 224, **C**), 417.4 (d, J_{HP} = 238, **D**).

Preparation of [Ag{$Mo_2Cp(\mu$-κ^1:κ^1:κ^1,η^5-PC_5H_4)$(CO)_2(\eta^6$-HR*)}$_2$][PF_6] (19). A dichloromethane solution (4 mL) of [$Ag(PPh_3)(THT)_n$][PF_6] (0.037 mmol) was prepared in situ by stirring [$AgCl(PPh_3)$]$_4$ (0.015 g, 0.037 mequiv) and $TlPF_6$ (0.013 g, 0.037 mmol) in the presence of THT (0.05 mL, excess) for 10 min. The solution was filtered using a canula and added to a solution of compound **3** (0.023 g, 0.035 mmol), and the mixture was stirred for 1 min to give a green solution. Solvent was then removed under a vacuum; the residue was washed with petroleum ether (3 × 5 mL), then extracted with dichloromethane (10 mL), and the extract filtered with a canula. Removal of solvent from the filtrate gave compound **18** as a reasonably pure green-emerald solid. All attempts to further purify this solid, however, resulted in its progressive decomposition. IR and ^{31}P NMR data for this compound are given in Table 2.

Preparation of [Ag{$Mo_2Cp(\mu$-κ^1:κ^1:κ^1,η^5-PC_5H_4)$(CO)_2(\eta^6$-HR*)}$_2$][BAr′$_4$) (19′). A dichloromethane solution (4 mL) of [$Ag(PPh_3)(THT)_n$][BAr′$_4$) (0.037 mmol) was prepared in situ by stirring [$AgCl(PPh_3)$]$_4$ (0.015 g, 0.037 mequiv) and Na(BAr′$_4$) (0.033 g, 0.037 mmol) in the presence of THT (0.05 mL, excess) for 10 min. The solution was filtered using a canula and added to a solution of compound **3** (0.023 g, 0.035 mmol), and the mixture was stirred for 1 min to give a green solution. Workup as described for **19** yielded compound **19′** as a green-emerald microcrystalline solid (0.030 g, 75%). Anal. Calcd for $C_{92}H_{90}AgBF_{24}Mo_4O_4P_2$: C, 48.46; H, 3.98. Found: C, 48.03; H, 4.29. ^{1}H NMR (400.13 MHz): δ 7.70 (m, 8H, Ar′), 7.56 (s, br, 4H, Ar′), 5.59 (s, 5H, Cp), 5.35 (s, br, 4H, C_6H_3 and C_5H_4), 5.15, 5.07, 4.18 (3m, 3 × 1H, C_5H_4), 1.26 (s, 27H, ^{t}Bu).

Preparation of [Ag{$Mo_2Cp_2(\mu_3$-PH)$(CO)_2(\eta^6$-HR*)}$_2$][BAr′$_4$) (20). A dichloromethane solution (4 mL) of [$Ag(PPh_3)(THT)_n$]-(BAr′$_4$) (0.042 mmol) was prepared in situ by stirring [$AgCl(PPh_3)$]$_4$ (0.015 g, 0.042 mequiv) and Na(BAr′$_4$) (0.037 g, 0.042 mmol) in the presence of THT (0.05 mL, excess) for 10 min. The solution was filtered using a canula and added to a solution of compound **4** (0.023 g, 0.035 mmol) at 213 K, and the mixture was stirred for 1 min to give a blue-violet solution, then allowed to reach room temperature for 1 h to give a green solution. Solvent was then removed under a vacuum; the residue was washed with petroleum ether (3 × 5 mL) then extracted with dichloromethane/petroleum ether (1/1) and the extracts chromatographed on alumina (activity IV) at 288 K. Elution with the same solvent mixture gave a green fraction yielding, after removal of solvents, compound **20** as a rather unstable green solid (0.025 g, 63%). All attempts to further purify this solid, however, resulted in its progressive decomposition. ^{31}P NMR: δ 474.4 (dd, J_{HP} = 215, $J^{109}_{AgP} \approx J^{107}_{AgP}$ = 100, μ_3-PH). ^{1}H NMR: δ 11.75 (d, J_{HP} = 217, 2H, μ_3-PH), 7.72 (m, 8H, Ar′), 7.56 (s, br, 4H, Ar′), 5.50 (s, 10H, Cp), 5.12 (s, br, 6H, C_6H_3), 4.92 (d, br, J_{HP} = 5, 10H, Cp), 1.17 (s, 54H, ^{t}Bu).

Preparation of [Cu{$Mo_2Cp_2(\mu$-κ^1:κ^1:κ^1,η^6-PR*)$(CO)_2$}$_2$][PF_6] (21). A dichloromethane solution (4 mL) of compound **1** (0.025 g, 0.038 mmol) and [$Cu(NCMe)_4$]PF_6 (0.008 g, 0.022 mmol) was stirred at room temperature for 5 min to give a deep red solution. Workup as described for **16** yielded compound **21** as a very air-sensitive red solid (0.020, 69%). ^{1}H NMR (400.13 MHz): δ 5.89 (s, br, 2H, C_6H_2), 5.81 (s, br, 2H, C_6H_2), 5.60, 5.47, 5.43, 5.31 (4s, br, 4 × 5H, Cp), 1.36, 1.35 (2s, 2 × 9H, ^{t}Bu), 1.32, 1.24 (2s, 2 × 18H, ^{t}Bu).

X-ray Crystal Structure Determination for Compounds 6, 10, and 17. Data collection was performed at 100 K on a Nonius KappaCCD single-crystal diffractometer, using Mo Kα radiation. Images were collected at a 35, 50, and 45 mm fixed crystal-detector distances, respectively, using the oscillation method, with 1, 0.5, and 0.7° oscillation and 50, 60, and 100 s exposure time per image, respectively. Data collection strategy was calculated with the program *Collect*.[42] Data reduction and cell refinements were performed with the programs *HKL Denzo* and *Scalepack*.[43] Semiempirical absorption corrections were applied using the program SORTAV.[44] Using the program suite WinGX,[45] the structures were solved by Patterson interpretation and phase expansion using SHELXL97[46] and refined with full-matrix least-squares on F^2 using SHELXL97. All non-hydrogen atoms were refined anisotropically, except those involved in disorder, and hydrogen atoms were geometrically placed and refined isotropically using a riding model. Crystallographic data and structure refinement details are collected in Table 9. Compound **6** was found to crystallize with two molecules of dichloromethane, one of them highly disordered and placed on a symmetry element. The latter could not be satisfactorily modeled; therefore, the SQUEEZE procedure,[47] as implemented in PLATON,[48] was applied. Moreover atoms C(11) and C(18) were refined isotropically to prevent their temperature factors from becoming nonpositive definite, and atoms H(16) and

dx.doi.org/10.1021/ic501376v | *Inorg. Chem.* 2014, 53, 10325−10339

H(18) were located in the Fourier map and refined isotropically. The structure of compound **10** was solved with the SIR92 program;[49] two molecules of dichloromethane were present in the unit cell, and a number of carbon atoms had to be refined isotropically; the most intense residuals of electron density were located near the mercury atoms. For compound **17**, two molecules of dichloromethane were also present in the unit cell, along with a third molecule of a nonidentified solvent, to which the SQUEEZE procedure was applied.

X-ray Crystal Structure Determination for Compounds 9 and 18. Data collection was performed at 100 K on a Kappa-Appex-II Bruker diffractometer using graphite-monochromated Mo Kα radiation at 100 K. The software APEX[50] was used for collecting frames with ω/ϕ scans measurement method. The SAINT software was used for data reduction,[51] and multiscan absorption corrections were applied with SADABS.[52] Structure solution and refinements were performed in general as described above. For compound **9**, the asymmetric unit contained three molecules of the complex, a toluene molecule, and a second molecule of a nonidentified solvent, to which the SQUEEZE procedure was applied. Due to poor quality of the data, not all non-H atoms could be freely refined anisotropically: an important number of atoms had to be refined anisotropically in combination with the instructions DELU and SIMU, and three carbon atoms had to be refined isotropically to prevent their temperature factors from becoming nonpositive definite. Upon convergence, the strongest residual peaks were located near the gold atoms. For compound **18**, the structure was solved by direct methods using SIR92, and three molecules of diethyl ether were present in the asymmetric unit. Moreover, a number of carbon atoms also had to be refined anisotropically in combination with the instructions DELU and SIMU. Atoms H(1) and H(2) were located in the Fourier maps and refined isotropically.

X-ray Crystal Structure Determination for Compounds 13b and 15d. Data collection was performed at 100 K on an Oxford Diffraction Xcalibur Nova single crystal diffractometer, using Cu Kα radiation. Images were collected at a 65 mm fixed crystal-detector distance, using the oscillation method, with 1° oscillation and variable exposure time per image (1.5−6.5 s for **13b**, 10−40 s for **15d**). The data collection strategy was calculated with the program CrysAlis Pro CCD.[53] Data reduction and cell refinements were performed with the program CrysAlis Pro RED.[53] Empirical absorption corrections were applied using the SCALE3 ABSPACK algorithm as implemented in the program CrysAlis Pro RED. Structure solution and refinements were in general performed as described above, except for **13b**, solved with SIR92. The atoms H(16) and H(18) in this complex were located in the Fourier maps and refined isotropically, and a molecule of an unidentified solvent was found to be present in the asymmetric unit, to which the SQUEEZE procedure was applied. Compound **15d** was found to crystallize with half a molecule of hexane placed on the symmetry operation $-x + 1, -y + 1, -z$. Moreover, two CF_3 groups, a cyclopentadienyl ligand, a methyl group of the mesityl ring and an isopropyl group of the phosphine ligand, were found to be disordered. The CF_3 groups were modeled over two positions with 0.5 occupancy factors and one of the cyclopentadienyl groups with occupancy factors of 0.6/0.40. Disorders involving the methyl and isopropyl groups could not be satisfactorily modeled. The P-bound H(1) atom was located in the Fourier map and refined isotropically.

■ ASSOCIATED CONTENT

Ⓢ Supporting Information

A CIF file containing full crystallographic data for compounds **6**, **9**, **10**, **13b**, **15d**, **17**, and **18** (CCDC 1005056 to 1005062). This material is available free of charge via the Internet at http://pubs.acs.org.

■ AUTHOR INFORMATION

Corresponding Authors

*E-mail: garciame@uniovi.es.

*E-mail: mara@uniovi.es.

Notes

The authors declare no competing financial interest.

■ ACKNOWLEDGMENTS

We thank the DGI of Spain (Project CTQ2012-33187) and the Consejería de Educación del Principado de Asturias and the Universidad de Oviedo for grants (to J.S, I.A., and B.A.). We also thank the X-ray units of the Universidad de Oviedo and Universidad de Santiago de Compostela for acquisition of diffraction data.

■ REFERENCES

(1) (a) Schmidbaur, H.; Schier, A. *Chem. Soc. Rev.* **2012**, *41*, 370. (b) Sculfort, S.; Braunstein, P. *Chem. Soc. Rev.* **2011**, *40*, 2741. (c) Pyykkö, P. *Inorg. Chim. Acta* **2005**, *358*, 4413. (d) Pyykkö, P. *Angew. Chem., Int. Ed.* **2004**, *43*, 4412.

(2) (a) Che, C.-M.; Lai, S.-W. *Gold Chem.* **2009**, 249. (b) Evans, R. C.; Douglas, P.; Winscom, C. J. *Coord. Chem. Rev.* **2006**, *250*, 2093. (c) Yam, V. W. W.; Lo, K. K. W. *Chem. Soc. Rev.* **1999**, *28*, 323.

(3) For some recent reviews see, for instance: (a) Wang, Y.-M.; Lackner, A. D.; Toste, F. D. *Acc. Chem. Res.* **2014**, *47*, 889. (b) Obradors, C.; Echavarren, A. M. *Acc. Chem. Res.* **2014**, *47*, 902. (c) Hashmi, A.; Stephen, K. *Acc. Chem. Res.* **2014**, *47*, 864. (d) Alcaide, B.; Almendros, P. *Acc. Chem. Res.* **2014**, *47*, 939.

(4) (a) Gimeno, M. C.; Laguna, A. In *Comprehensive Coordination Chemistry II*; McCleverty, J. A., Meyer, T. J., Eds.; Elsevier: Oxford, U. K., 2004; Vol. *6*, Chapter 7. (b) Salter, I. D. In *Comprehensive Organometallic Chemistry*, 2nd ed.; Abel, E. W., Stone, F. G. A., Wilkinson, G., Eds.; Pergamon: Oxford, U. K., 1995; Vol. *10*, Chapter 5.

(5) Huttner, G.; Knoll, K. *Angew. Chem., Int. Ed.* **1987**, *26*, 743.

(6) Deeming, A. J.; Doherty, S.; Day, M. W.; Hardcastle, K. I.; Minassian, H. *J. Chem. Soc., Dalton Trans.* **1991**, 1273.

(7) Haupt, H.-J.; Schwefer, M.; Egold, H.; Flörke, U. *Inorg. Chem.* **1995**, *34*, 5461.

(8) Vogel, U.; Sekar, P.; Ahlrichs, R.; Huniar, U.; Scheer, M. *Eur. J. Inorg. Chem.* **2003**, 1518.

(9) Alvarez, M. A.; García, M. E.; González, R.; Ramos, A.; Ruiz, M. A. *Inorg. Chem.* **2011**, *50*, 7894.

(10) (a) Scheer, M.; Himmel, D.; Kuntz, C.; Zhan, S.; Leiner, E. *Chem.—Eur. J.* **2008**, *14*, 9020. (b) Sánchez-Nieves, J.; Sterenberg, B. T.; Udachin, K. A.; Carty, A. J. *Can. J. Chem.* **2004**, *82*, 1507. (c) Sánchez-Nieves, J.; Sterenberg, B. T.; Udachin, K. A.; Carty, A. J. *Can. J. Chem.* **2003**, *81*, 1149. (d) Lang, H.; Zsolnai, L.; Huttner, G. *J. Organomet. Chem.* **1985**, *282*, 23.

(11) (a) García, M. E.; Riera, V.; Ruiz, M. A.; Sáez, D.; Hamidov, H.; Jeffery, J. C.; Riis-Johannessen, T. *J. Am. Chem. Soc.* **2003**, *125*, 13044. (b) Amor, I.; García, M. E.; Ruiz, M. A.; Sáez, D.; Hamidov, H.; Jeffery, J. C. *Organometallics* **2006**, *25*, 4857.

(12) Alvarez, M. A.; Amor, I.; García, M. E.; García-Vivó, D.; Ruiz, M. A.; Suárez, J. *Organometallics* **2010**, *29*, 4384.

(13) Alvarez, M. A.; Amor, I.; García, M. E.; García-Vivó, D.; Ruiz, M. A. *Inorg. Chem.* **2007**, *46*, 6230.

(14) (a) Alvarez, M. A.; Amor, I.; García, M. E.; Ruiz, M. A.; Suárez, J. *Organometallics* **2012**, *31*, 2749. (b) Alvarez, M. A.; García, M. E.; Ruiz, M. A.; Suárez, J. *Angew. Chem., Int. Ed.* **2011**, *50*, 6383.

(15) Alvarez, M. A.; Amor, I.; García, M. E.; Ruiz, M. A. *Inorg. Chem.* **2008**, *47*, 7963.

(16) Greenwood, N. N.; Earnshaw, A. *Chemistry of the Elements*, 2nd ed.; Butterworths-Heinemann: Oxford, U. K., 1988; Chapter 28.

(17) Pethe, J.; Maichle-Mössmer, C.; Strähle, J. *Z. Anorg. Allg. Chem.* **1997**, *623*, 1413.

(18) Hartung, H.; Walter, B.; Baumeister, U.; Bottcher, H.-C.; Krung, A.; Rosche, F.; Jones, P. G. *Polyhedron* **1992**, *11*, 1563.

(19) (a) Teets, T. S.; Neumannn, M. P.; Nocera, D. G. *Chem. Commun.* **2011**, *47*, 1485. (b) Teets, T. S.; Lutterman, D. A.; Nocera, D. G. *Inorg. Chem.* **2010**, *49*, 3035. (c) Cook, T. R.; Esswein, A. J.; Nocera, D. G. *J. Am. Chem. Soc.* **2007**, *129*, 10094.

(20) Carty, A. J.; MacLaughlin, S. A.; Nucciarone, D. In *Phosphorus-31 NMR Spectroscopy in Stereochemical Analysis*; Verkade, J. G., Quin, L. D., Eds.; VCH: Deerfield Beach, FL, 1987; Chapter 16.
(21) Braterman, P. S. *Metal Carbonyl Spectra*; Academic Press: London, U. K., 1975.
(22) Alvarez, B.; Alvarez, M. A.; Amor, I.; García, M. E.; García-Vivó, D.; Ruiz, M. A.; Suárez, J. *Inorg. Chem.* **2012**, *51*, 7810.
(23) Fischer, P. J.; Krohn, K. M.; Mwenda, E. T.; Young, V. G., Jr. *Organometallics* **2005**, *24*, 5116.
(24) Sculfort, S.; Welter, R.; Braunstein, P. *Inorg. Chem.* **2010**, *49*, 2372.
(25) Bauer, J.; Braunschweig, H.; Dewhurst, R. D. *Chem. Rev.* **2012**, *112*, 4329.
(26) Bell, N. A.; March, L. A.; Nowell, I. W. *Inorg. Chim. Acta* **1989**, *156*, 201.
(27) Ciplys, A.; Geue, R. J.; Snow, M. R. *J. Chem. Soc., Dalton Trans.* **1976**, 35.
(28) Cordero, B.; Gómez, V.; Platero-Prats, A. E.; Revés, M.; Echeverría, J.; Cremades, E.; Barragán, F.; Alvarez, S. *Dalton Trans.* **2008**, 2832.
(29) (a) Bueno, C.; Churchill, M. R. *Inorg. Chem.* **1981**, *20*, 2197. (b) Cano, M.; Criado, R.; Gutierrez-Puebla, E.; Monge, A.; Pardo, M. P. *J. Organomet. Chem.* **1985**, *292*, 375. (c) Cano, M.; Campo, J. A.; Pinilla, E.; Monge, A.; Pichon, R.; Salaun, J.-Y.; L'Haridon, P.; Szymoniak, J.; Kubicki, M. M. *Inorg. Chim. Acta* **1995**, *228*, 251.
(30) Arif, A. M.; Cowley, A. H.; Norman, N. C.; Orpen, A. G.; Pakulski, M. *Organometallics* **1988**, *7*, 309.
(31) Cano, M.; Campo, J. A.; Le Gall, J.-Y.; Pichon, R.; Salaun, J.-Y.; Kubicki, M. M. *Inorg. Chim. Acta* **1992**, *193*, 207.
(32) One bond $^{31}P-^{199}Hg$ couplings are strongly dependent on the chemical environments of the P and Hg atoms and display a very wide range of shifts. For instance, P−Hg couplings in linear complexes $[HgX(PMe_3)]$ fall in the range 1750−7850 Hz depending on X (halide or related ligand). See: Verkade, J. G.; Mosbo, J. A. In *Phosphorus-31 NMR Spectroscopy in Stereochemical Analysis*; Verkade, J. G., Quin, L. D., Eds.; VCH: Deerfield Beach, FL, 1987; Chapter 13.
(33) Malish, W.; Hirth, U. A.; Bright, T. A.; Käb, H.; Ertel, T. J.; Hückmann, S.; Bertagnolli, H. *Angew. Chem., Int. Ed. Engl.* **1992**, *31*, 1525.
(34) A general trend established for $^2J_{XY}$ in complexes of the type $[MCpXYL_2]$ is that $|J_{cis}| > |J_{trans}|$. See, for instance: (a) Jameson, C. J. In *Phosphorus-31 NMR Spectroscopy in Stereochemical Analysis*; Verkade, J. G., Quin, L. D., Eds.; VCH: Deerfield Beach, FL, 1987; Chapter 6. (b) Wrackmeyer, B.; Alt, H. G.; Maisel, H. E. *J. Organomet. Chem.* **1990**, *399*, 125.
(35) (a) Carriedo, G. A.; Howard, J. A. K.; Marsden, K.; Stone, F. G. A.; Woodward, P. *J. Chem. Soc., Dalton Trans.* **1984**, 1589. (b) Carriedo, G. A.; Riera, V.; Sanchez, G.; Solans, X.; Labrador, M. *J. Organomet. Chem.* **1990**, *391*, 431.
(36) Armarego, W. L. F.; Chai, C. *Purification of Laboratory Chemicals*, 5th ed.; Butterworth-Heinemann: Oxford, U. K., 2003.
(37) Usón, R.; Laguna, A.; Laguna, M. *Inorg. Synth.* **1989**, *26*, 85.
(38) Braunstein, P.; Lehrer, H.; Matt, D. *Inorg. Synth.* **1990**, *27*, 218.
(39) Cariati, F.; Naldini, L. *Gazz. Chim. Ital.* **1965**, *95*, 201.
(40) Gladysz, J. A.; Williams, G. M.; Tom, W.; Johnson, D. L.; Parker, D. W.; Selover, J. C. *Inorg. Chem.* **1979**, *18*, 553.
(41) Yakelis, N. A.; Bergman, R. G. *Organometallics* **2005**, *24*, 3579.
(42) *Collect*; Nonius BV: Delft, The Netherlands, 1997−2004.
(43) Otwinowski, Z.; Minor, W. *Methods Enzymol.* **1997**, *276*, 307.
(44) Blessing, R. H. *Acta Crystallogr.* **1995**, *A51*, 33.
(45) Farrugia, L. J. *J. Appl. Crystallogr.* **1999**, *32*, 837.
(46) Sheldrick, G. M. *Acta Crystallogr.* **2008**, *A64*, 112.
(47) Van der Sluis, P.; Spek, A. L. *Acta Crystallogr.* **1990**, *A46*, 194.
(48) Spek, A. L. *PLATON, A Multipurpose Crystallographic Tool*; Utrecht University: Utrecht, The Netherlands, 2010.
(49) Altomare, A.; Cascarano, G.; Giacovazzo, C.; Guagliardi, A.; Burla, M. C.; Polidori, G.; Camalli, M. *J. Appl. Crystallogr.* **1994**, *27*, 435.
(50) *APEX 2*, version 2.0−1; Bruker AXS Inc: Madison, WI, 2005.
(51) *SMART & SAINT Software Reference Manuals*, version 5.051 (Windows NT version); Bruker Analytical X-ray Instruments: Madison, WI, 1998.
(52) Sheldrick, G. M. *SADABS, Program for Empirical Absorption Correction*; University of Göttingen: Göttingen, Germany, 1996.
(53) *CrysAlis Pro*; Oxford Diffraction Ltd.: Oxford, U. K., 2006.